Dynamic tracking of social variables

in simultaneous brain recordings of socially interacting monkeys

Sini Simon, Debdyuti Bhadra, Shubhankar Saha,

Surbhi Munda, Jhilik Das & SP Arun*

Centre for Neuroscience, Indian Institute of Science, Bangalore 560012

*Correspondence to: sparun@iisc.ac.in

ABSTRACT

Primates are deeply social, but the underlying neural basis has been elusive because brain activity is often recorded in artificially constrained conditions. Here, we recorded wireless neural activity simultaneously from two macaque monkeys interacting socially in a natural setting. Neural activity in each monkey encoded key social variables such as allogrooming state, partner identity and joint movements. Surprisingly, neurons in the high-level visual cortex of each monkey continuously tracked a social favor signal, i.e. net duration of allogrooming given versus received, providing a neural basis for grooming reciprocity. In both monkeys, while grooming their partner, neural activity was predicted better by the partner's joints and his brain activity. Thus, the receiver of grooming drove the social interaction, not the groomer. Taken together, our findings elucidate the rich and dynamic neural basis of primate social interactions in an ecologically valid setting.

INTRODUCTION

Primates are deeply social, and these social interactions evoke widespread brain activity (Sliwa and Freiwald, 2017; Shepherd and Freiwald, 2018; Wittmann et al., 2018; Gilbert et al., 2021; Deen et al., 2023; McMahon and Isik, 2023). However, understanding the neural basis of social interactions has been technically challenging, because brain recordings are often feasible only under highly artificial, restrained conditions (Fan et al., 2021). Under these conditions, brain activity has been recorded from monkeys interacting with social partners, showing tracking of the partners' actions, reward states and strategies (Yoshida et al., 2012; Ong et al., 2021; Haroush and Williams, 2015; Chang et al., 2013; Báez-Mendoza et al., 2021). Likewise, brain activity has been recorded simultaneously from socially interacting monkeys, showing interbrain synchrony (Tseng et al., 2018; Gilbert et al., 2021) and also modulation by the partner's actions (Fujii et al., 2007, 2009). Similar observations have been made in mice (Kingsbury et al., 2019; Zhang et al., 2025), bats (Zhang and Yartsev, 2019; Rose et al., 2021) and even humans (Stephens et al., 2010; Kinreich et al., 2017).

With advances in wireless neural recording technology, brain activity has been recorded under increasingly unrestrained and more natural conditions (Roy and Wang, 2012; Schwarz et al., 2014; Berger et al., 2020; Hansmeyer et al., 2023). Indeed, a recent study has used wireless brain recordings in monkeys freely interacting with a social partner, to find clusters of neural activity corresponding to various behavioral and social states (Testard et al., 2024). These advances have prompted calls for concerted efforts to study brain activity in natural and social behaviors (Testard et al., 2021; Cisek and Green, 2024; Parodi et al., 2025).

A deeper understanding of the neural basis of primate social interactions will require overcoming several challenges. First, brain activity must be recorded wirelessly and simultaneously from socially interacting monkeys in a natural setting without any constraints. This requires not only seamless integration of two wireless recording systems but also ensuring social compatibility of the two monkeys to minimize the risk of aggressive encounters that could damage their implants. Second, since brain activity during social interactions is widespread, multiple high-level sensory and motor regions must be monitored simultaneously. Finally, for brain activity during social interactions to be more interpretable, it must be combined with brain recordings in a more controlled setting where basic sensory and motor responses can be characterized.

Here, we performed simultaneous wireless brain recordings from high-level visual and motor regions of two socially compatible monkeys while they interacted freely in a naturalistic setting without any constraints. We also recorded brain activity in each monkey separately while he performed visual and motor tasks on a touchscreen. We targeted the inferior temporal (IT) cortex, a region critical for object recognition that is also sensitive to social stimuli (Morin et al., 2015; Testard et al., 2024), the ventral premotor cortex (PMv), which contains mirror neurons sensitive to social gaze and intention (Rizzolatti and Craighero, 2004) and the ventrolateral prefrontal cortex (PFC), a region involved in executive control and social behaviors (Chang et al., 2013; Báez-Mendoza et al., 2021; Franch et al., 2024). We investigated several fundamental questions. First, does brain activity in each animal encode key variables important for social interactions? Second, is neural activity in both brains coupled during a social interaction: does the groomer's neural activity drive the receiver's neural activity or vice-versa?

RESULTS

To investigate the neural basis of social behavior, we implanted two socially compatible male bonnet macaque monkeys (M1 and M2), each with 256 microelectrodes spanning high-level visual and motor regions (visual regions: inferior temporal cortex - IT; motor regions: ventral premotor cortex - PMv and ventrolateral prefrontal cortex – PFC; see Methods). We recorded brain activity wirelessly and simultaneously from both monkeys while they interacted freely without any constraints. In order to interpret brain activity as being of sensory or motor origin during the social interaction, we also recorded brain activity from each monkey separately while he performed a visual task and a motor task on a custom-designed touchscreen workstation with eye tracking capabilities (Jacob et al., 2021). In the visual task, each monkey had to fixate on face and body images of himself, his partner, and another unrelated monkey. In the motor task, each monkey had to touch targets appearing on a touchscreen with his left or right hand.

During the social interaction session, the two monkeys took turns grooming each other, interspersed with transition periods of no grooming (Figure 1A). Brain activity recorded during this entire session from the visual and motor regions showed rich dynamics (Figure 1B) that we did our best to elucidate in the sections below.

We hypothesized that, during the social interaction, neural activity in each monkey should keep track of important social variables, such as the time spent in giving versus receiving grooming, the identity of the social partner and his movements. We also hypothesized that there should be dynamic interbrain coupling during the social interaction, which we sought to elucidate using predictive modeling.

81 **Social interaction & grooming reciprocity**

82 The two male monkeys were socially compatible, with M2 dominant over M1. This
83 dominance was also evident during the social interaction session in several ways: M2
84 mounted M1 at the start of the interaction, moved confidently around M1 brushing against
85 him, while M1 remained stationary, M2 groomed M1's face and handled M1's implant to
86 orient his head, and initiated grooming transitions. Likewise, M1 showed subordination to
87 M2 in several ways, such as frequent lip-smacking, remaining stationary with his head
88 down when M2 moved around him, grooming M2's body more often than the face, and
89 never handling M2's implant. During the social interaction session, M2 groomed M1 first,
90 M1 then groomed M2 and finally, M2 groomed M1 – all using stereotypical allogrooming
91 behaviors (Figure 1A). While being groomed, both monkeys often used referential
92 gestures to indicate the body part that they wished to be groomed, and their partner often
93 responded immediately by grooming that body part (Video S1). Such referential gestures
94 have also been observed in the wild (Sinha, 1998; Gupta and Sinha, 2016).

95 Interestingly, M2 groomed M1 for a total of 244 s across 8 bouts, and M1 groomed
96 M2 also for a similar total duration, of 230 s across 4 bouts (Figure 1C). Thus, both
97 monkeys groomed each other for roughly equal durations, demonstrating an almost
98 perfect reciprocity of grooming, in keeping with previous observations (Adiseshan et al.,
99 2011; Onishi et al., 2013; Molesti and Majolo, 2017; Testard et al., 2024).

100 What could be the neural basis for this remarkable reciprocity? One possibility is
101 that each monkey could create a running "social favor" signal, which tracks the net social
102 favor (given minus received). In this case, social favor is quite simply, net duration of
103 grooming (give – receive) or grooming surplus (Figure 1D) – but this could be more

complex in the case of more sophisticated social interactions. A positive value of the signal indicates that the monkey has given more grooming than he has received. Presumably, when this signal reaches a high enough value, the monkey might decide to stop grooming and wait for his partner to reciprocate. Conversely, a negative value would mean that the monkey has received more grooming than he has given. Likewise, when the signal is sufficiently negative, the monkey might decide to stop receiving grooming and start grooming his partner. Critically, the grooming surplus signal will be opposite in sign for the two monkeys: when M1 is grooming M2, grooming surplus of M1 would increase whereas the grooming surplus of M2 would decrease. Further, we speculated that, since neural activity in motor regions would be directly involved in grooming behavior, such a social favor signal might be reflected in high-level visual regions (or other non-motor regions) rather than in motor regions, to avoid interference with any ongoing motor movements.

In our social interaction session, since at first M2 groomed M1, then M1 groomed M2 and then M2 groomed M1 again, the social favor (grooming surplus) signal for M1 would decrease at first, increase and then decrease again. Conversely, the social favor signal for M2 should increase at first, decrease and then increase again.

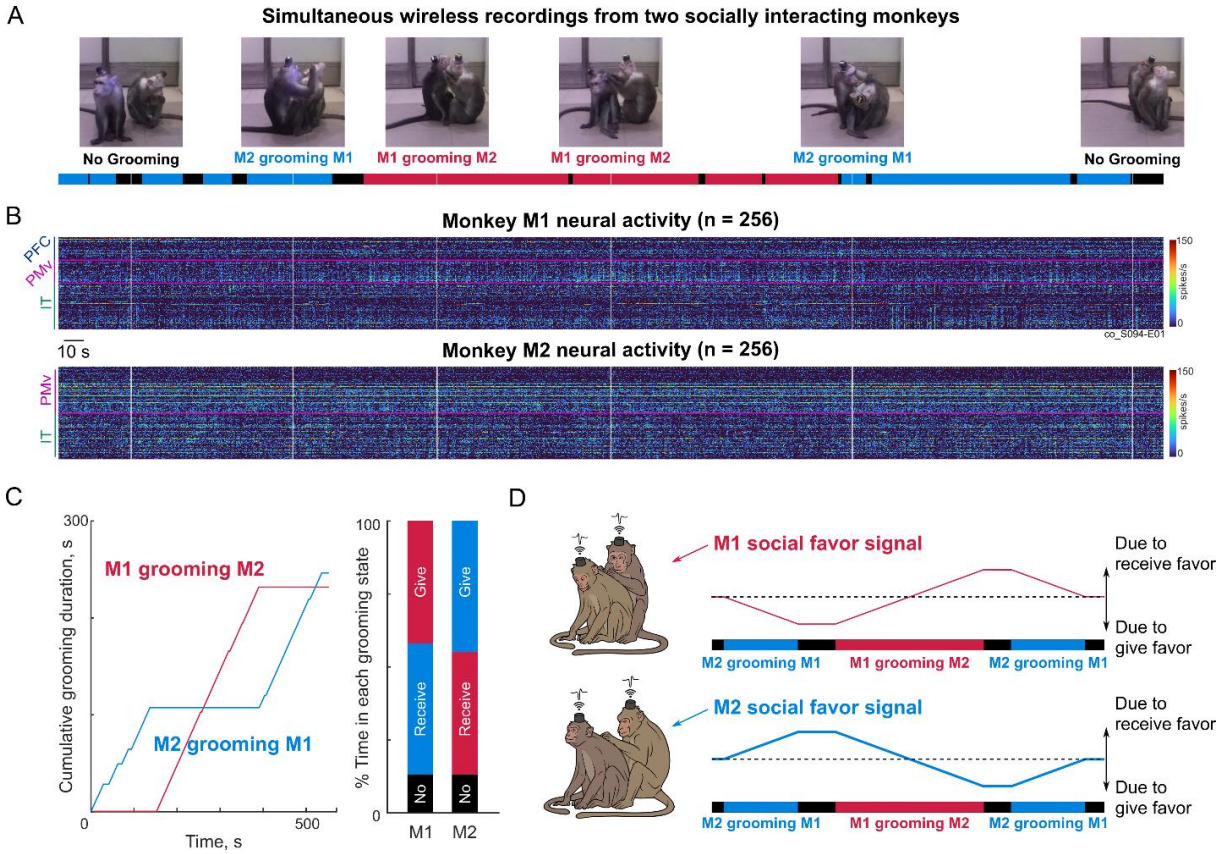

Figure 1: Simultaneous wireless brain recordings in socially interacting monkeys

(A) Timeline of the social interaction session with two monkeys, with example frames (*white lines*) illustrating the three types of grooming behavior observed: No grooming (*black*), M2 grooming M1 (*blue*) and M1 grooming M2 (*red*).

(B) Firing rates in 0.5 s bins of all 512 neurons recorded wirelessly and simultaneously from both monkeys, with *white vertical lines* corresponding to the example frames in (A), and *pink horizontal lines* segregating brain regions (PFC, PMv, IT in M1; PMv, IT in M2).

(C) *Left:* Cumulative duration of each type of grooming as a function of time: M2 grooming M1 (*blue*) and M1 grooming M2 (*red*). *Right:* Percentage of total session time spent by each monkey in grooming (marked *giving*), receiving grooming (marked *receiving*) and neither (marked *no*). Note that giving grooming for one monkey will be receiving grooming for the other, so the two bars are redundant. Both monkeys showed an near-perfect grooming reciprocity, i.e. groomed each other for almost equal durations.

(D) Schematic of how monkeys' brains might achieve reciprocity. Consider a session in which first M2 grooms M1, then M1 grooms M2 and then M2 grooms M1. We reasoned that each monkey could create a "social favor" signal representing the net duration spent in giving minus receiving grooming. This signal is positive if he has given more than he has received and negative if has received more than he has given. *Top:* For monkey M1, the social favor signal goes negative at first (since his partner is grooming him), then becomes positive and goes down to zero. *Bottom:* For monkey M2, the social favor signal goes positive initially (since he is grooming his partner), becomes negative and then rises back to zero.

148 **Social favor signals as a neural basis for grooming reciprocity**

149 To investigate whether the grooming surplus (social favor) signal in each monkey
150 is represented in the population activity of each brain region, we plotted this signal along
151 with the mean firing rate for each region. Since these quantities are likely to be slow
152 varying signals, we plotted the firing rates and grooming surplus in 30 s bins. We obtained
153 qualitatively similar results on varying this choice.

154 Strikingly, the average neural activity in IT of monkey M1 was strongly correlated
155 with his own grooming surplus signal (r = 0.65, p < 0.005; Figure 2A, *upper panel*).
156 Likewise, the average neural activity in IT of monkey M2 mirrored his own grooming
157 surplus signal (r = 0.5, $p < 0.05$; Figure 2A, *lower panel*). This correlation was not present
158 in the average neural activity of PMv neurons (correlation: r = 0.02, p = 0.94 for M1; r =
159 0.33, p = 0.17 for M2), nor in the average neural activity of PFC (r = 0.17, p = 0.5).

160 To investigate this further at the level of single neurons, we repeated this analysis
161 on the firing rates of individual neurons. Across both monkeys, a substantial fraction of IT
162 neurons (21%, 51 of 243 neurons) showed a significant positive correlation (p < 0.05) with
163 the grooming surplus signal, while only 2% (6/243) showed a significant negative
164 correlation (Figure 2B). In PMv, we observed fewer neurons (9% i.e. 16/185) with
165 significant positive correlation and 3% (5/185) with significant negative correlation (Figure
166 2C, *left*). We found roughly equal proportions of neurons with positive and negative
167 correlations with grooming surplus in PFC (positive correlation: 15% i.e. 9 of 61 neurons;
168 negative correlation: 21% i.e., 13/61; Figure 2C, *right*). Thus, all three regions contained
169 neurons that tracked the grooming surplus. Across the entire population of neurons, both
170 IT and PMv neurons showed a significant positive average correlation with the grooming

171 surplus signal (Figure 2D). By contrast, PFC neurons did not show a significant correlation
172 with grooming surplus (Figure 2D). The grooming surplus correlation was strongest on
173 average in IT, followed by PMv, then by PFC (Figure 2D).
174
175 **Unique encoding of grooming surplus compared to other variables**
176 The above correlations with grooming surplus could arise from simpler differences
177 in overall firing while giving and receiving grooming. Likewise, animals might keep track
178 of grooming reciprocity by counting the number of times groomed, instead of the total
179 duration. We therefore created a number of possible alternative factors that could explain
180 the temporal variation in firing rates observed in single neurons. For each factor, we
181 calculated the average correlation, and also its partial correlation with neural firing after
182 removing all the other factors. This revealed that grooming surplus had the highest partial
183 correlation with IT neurons even after removing all other factors (Section S2). Similarly,
184 grooming state had the strongest influence on PMv neurons even after removing all other
185 factors (Section S2). Interestingly, none of these factors were strongly encoded by PFC
186 neurons (Section S2), but this null result is also limited by the fact that we only sampled
187 PFC in one monkey.
188 We conclude that neural activity in IT closely tracks social favor (grooming surplus)
189 signals in both monkeys. This unusual correspondence suggests that IT cortex helps
190 maintain grooming reciprocity, or at the very least, reflects this signal after it is generated
191 in other brain regions.
192

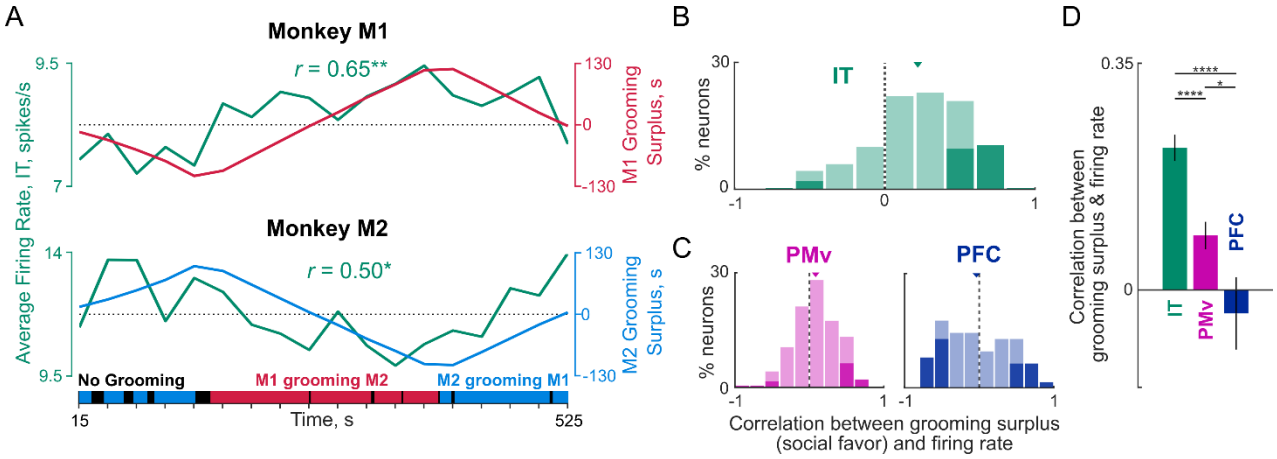

Figure 2. Reciprocity of grooming and its neural basis

(A) *Top:* Grooming surplus (social favor) signal for M1 (*red*), defined as the net duration of grooming (give – receive), overlaid with the average firing rate across IT neurons in M1 (*green*), calculated in 30 s bins. The correlation between the two signals is depicted in green, with asterisks showing statistical significance (*** is $p < 0.0005$).
Bottom: Grooming surplus (social favor) signal for M2 (*blue*) overlaid with the average
firing rate of IT neurons in M2 (*green*).

(B) Histogram of correlation between firing rates of neurons in each brain region with the respective grooming surplus (social favor) signal pooled across both monkeys for IT (*green*). Dark bars represent statistically significant correlations ($p < 0.05$), and the inverted triangle above the histogram represents the population mean.

(C) Same as (C) but for PMv (*left panel, purple*) and PFC (*right panel, blue*).

(D) Bar plot of average correlation (mean ± s.e.m across neurons, pooled across monkeys) with grooming surplus across neurons in each region. Asterisks indicate statistical significance of comparisons between brain regions (**** is $p < 0.00005$, * is $p < 0.05$, rank-sum test across correlation coefficients of neurons in the respective brain regions).

214 **Neural encoding of grooming state during social interaction**

215 Social interactions involve not only tracking the relative duration of social favors
216 like grooming, but also tracking of the ongoing grooming state. We therefore wondered
217 whether the neural activity in the recorded brain regions encodes these grooming states.
218 To start with, we plotted the average firing rate of each neuron when each monkey
219 groomed his partner (i.e. giving grooming) against when it received grooming from his
220 partner (i.e. receiving grooming). This revealed a heterogeneous pattern across neurons
221 in each brain region (Figure 3A), with some neurons showing consistent increases, some
222 showing decreases, and others showing no change in activity (Figure 3B).

223 In both monkeys, the average firing rate in IT and PMv showed an increase in the
224 giving grooming state compared to other conditions (Figure 3C). The increased PMv
225 activity while grooming the partner presumably reflects the greater amount of
226 movements involved during these bouts. Indeed, we found that the neurons that showed
227 increased activity during the touchscreen-based motor task also showed greater activity
228 while giving compared to receiving grooming (Section S1). Likewise, the increased IT
229 activity during giving grooming could be due to increased visual inputs during giving
230 grooming. Indeed, we found that neurons that showed increased activity during a fixation
231 task showed a larger difference in activity during giving vs receiving grooming (Section
232 S1).

233 The increased firing rates during giving compared to receiving grooming is
234 interesting, but to be expected since there is greater sensory and motor engagement for
235 the animal when it is grooming his partner. However, we observed an opposite pattern in
236 the local field potentials: there was greater LFP power in both IT and PMv while receiving

237 grooming compared to giving grooming in both monkeys (Section S3). We also observed
238 greater LFP power particularly in the alpha band in IT cortex during receiving grooming
239 (Section S3), presumably due to the monkey closing his eyes or relaxing while receiving
240 grooming. We speculate that the LFP activity could reflect greater inhibitory inputs while
241 receiving grooming, which in turn result in reduced neural firing.

242 Since neural responses are systematically different across grooming states, we
243 wondered whether grooming state can be reliably decoded from the neural activity
244 recorded during the social interaction. To this end, we trained a linear classifier on the
245 firing rates of neurons in successive 0.5 s time bins throughout the social session (Figure
246 3D). To avoid overfitting we used a 5-fold cross-validation procedure where the grooming
247 state in a given time bin was always predicted using a classifier that was never trained on
248 this bin. Decoding accuracy was consistently above chance for all grooming states
249 (Figure 3E) and in each brain region in both monkeys (Figure 3E).

250 To visualize the dynamics of grooming state decoding, we plotted the observed
251 grooming state throughout the session and compared it against the grooming state
252 predicted by the neural decoder of each monkey. This revealed a striking match between
253 the observed and predicted grooming state in both monkeys (Figure 3F). Finally, we
254 wondered whether the decoders trained on grooming states could predict the onset of the
255 grooming state using neural activity even before it was evident in behavior. This was
256 indeed the case: the decoder probability began to rise a few seconds before the onset of
257 giving or receiving grooming (Section S4).

258 Thus, each grooming state during the social interaction elicited distinct patterns of
259 neural activity in both visual and motor regions.

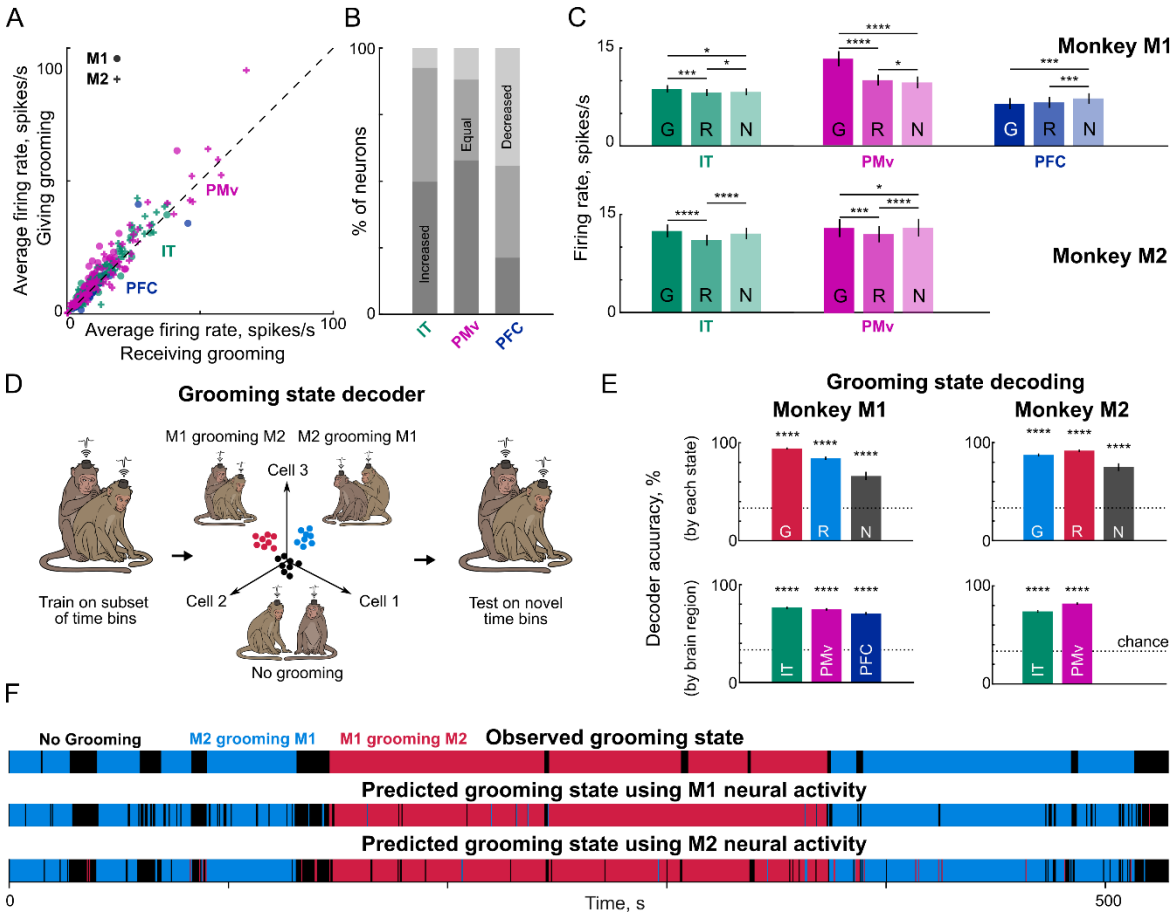

Figure 3: Neural tracking of grooming state during social interaction

(A) Average firing rate of all recorded neurons during Giving Grooming bouts plotted against the firing rate during Receiving Grooming bouts (*crosses*: M2 neurons; *dots*: M1 neurons; *green*: IT, *purple*: PMv, *blue*: PFC).

(B) Percentage of neurons in each brain region whose firing showed a significant increase (*dark*), decrease (*light*) or no significant change (*medium*), as identified using a rank-sum test on their firing rate in 0.5 s bins across the social session ($p < 0.05$).

(C) Average firing rate in monkey M1 (*top*) and M2 (*bottom*) across neurons in each brain region during different grooming bouts: giving grooming (G), receiving grooming (R) and no grooming (N). Error bars indicate s.e.m across neurons. Asterisks indicate statistical significance of comparing mean firing rates across different grooming behaviors (* is $p < 0.05$, ** is $p < 0.005$, etc., sign rank test across mean firing rates of neurons during each grooming bout).

(D) Schematic of grooming state decoding. We trained a linear classifier on the firing rates of neurons in 0.5 s bins labelled with their corresponding grooming state labels (M1 grooming M2, M2 grooming M1 or No grooming), and tested the classifier on novel time bins not seen during classifier training.

(E) *Top panel:* Grooming state decoding accuracy for each monkey, of a classifier trained on all neurons pooled across brain regions for each grooming state: Giving (G), Receiving (R) and No Grooming (N). Accuracy was calculated by pooling the results obtained from 5-fold cross-validation across folds. Error bars represent

s.e.m across 0.5 s time bins. Asterisks represent statistical significance of decoding accuracy (**** is $p < 0.00005$ using a chi-square test).
Bottom panel: Grooming state decoding accuracy for each monkey, of a classifier trained on each brain region (IT, PMv, PFC) pooled across grooming states. Asterisks represent statistical significance calculated as before.

(F) Observed grooming state for the entire session (*top*) shown along with predicted grooming state from the classifier trained on all neurons (across brain regions) from M1 (*middle*) and all neurons from M2 (*bottom*).

293 **Neural tracking of partner identity during social interaction**

294 Social interactions require not only tracking social favors and grooming state, but
295 also the identity of the current social partner. We therefore wondered whether neural
296 activity in both monkeys keep track of the identity of the partner during the social
297 interaction. Since neural activity during social interaction involves a multitude of signals,
298 we can only address this question by recording neural activity in a more controlled setting.
299 To this end, we recorded neural responses while each monkey performed a fixation task
300 (before the social session), where he viewed face & body images of himself, of his partner
301 and of a third unrelated monkey (Figure 4A). We then trained 3-way linear decoders to
302 decode individual monkey identity from the population activity recorded in each region
303 and tested them in the social session (Figure 4B).

304 In Monkey M1, neural activity in IT (but not PMv & PFC) correctly decoded his
305 partner i.e. Monkey M2 in all grooming states (Figure 4C), but particularly so while giving
306 grooming & no grooming. We speculate that this could be due to Monkey M1 tracking his
307 partner more closely, since he was the subordinate. We observed similar results in
308 Monkey M2: neural activity in IT (but not PMv) correctly decoded his partner i.e. Monkey
309 M1 across all grooming states (Figure 4D), with no obvious differences in decoding across
310 states. We did observe partner decoding changing dynamically over time (Section S5),
311 sometimes in ways related to the ongoing behavior (Section S9). We were also able to
312 decode the hand being used by each monkey during the social interaction, based on
313 using PMv responses in the motor task (Section S5).

Thus, neural activity in IT tracks the social partner consistently throughout the social interaction. Interestingly, we did not observe differences in partner decoding, even in grooming states where the monkey may not have been directly looking at his partner.

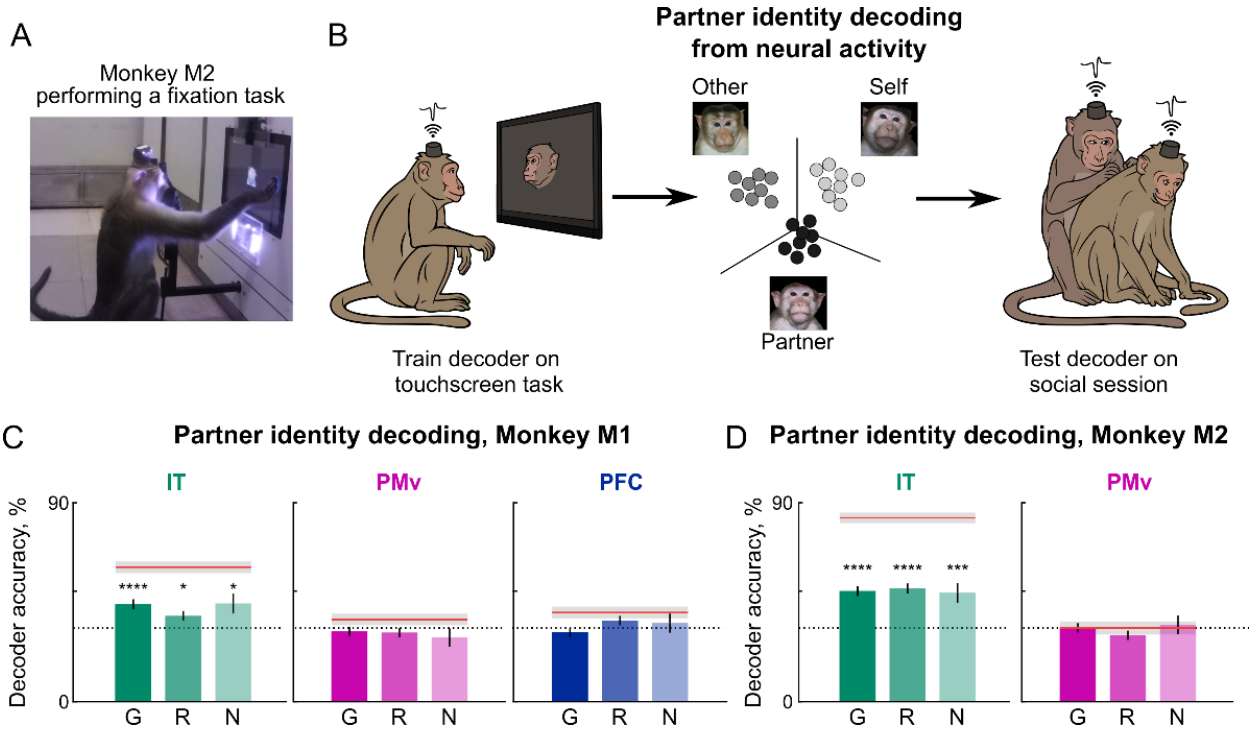

Figure 4: Neural tracking of partner identity during social interaction

(A) Example frame showing monkey M2 performing a fixation task.

(B) To investigate if each monkey's brain tracks his partner identity during the social interaction, we recorded neural responses while the monkey viewed photographs of himself, his partner and a third monkey on a touchscreen (*left panel*). We then trained a linear decoder to decode face identity (*middle panel*), and tested this decoder on neural activity during the social interaction (*right panel*).

(C) Partner identity decoding accuracy in IT, PMv and PFC neurons of Monkey M1 during the social interaction session, separated into the three grooming bouts: giving grooming (G), receiving grooming (R) and no grooming (N). Decoding accuracy was calculated in 0.5 s bins. Error bars represent s.e.m across all bins of that type. Decoding accuracy in the touchscreen task is also shown for reference (*red lines*, with *shaded regions* indicating s.e.m). Asterisks represent statistically significant decoding accuracy (* is $p < 0.05$, **** is $p < 0.00005$, chi-square test of correct and incorrect counts across all bins compared to the numbers expected by chance).

(D) Same as (C) but from the brain regions in Monkey M2.

336 **Neural tracking of self and partner movement during social interaction**

337 Social interactions inevitably involve closely coordinating one's own movements
338 with the partner depending on the nature of the ongoing interaction. We therefore
339 wondered whether neural activity in each monkey would track his own and his partner's
340 movements throughout the social interaction, and whether this would be dependent on
341 the nature of grooming interaction.

342 We had recorded videos from multiple views of the entire social interaction that
343 were synchronized to the wireless neural recordings. We selected the top view videos for
344 further analysis since most joints of both monkeys were clearly visible without occlusions
345 (Figure 5A). Since existing automated pose tracking algorithms did not work well to
346 separately identify the joints of the two interacting monkeys, we identified 20 key joints of
347 each monkey for manual annotation, and got them manually annotated and cross-verified
348 by a team of annotators (Figure 5A). We used the head, neck, left and right shoulder
349 positions as regressors, since these joints were visible in a large number of frames (we
350 obtained qualitatively similar results on varying this choice). We then built a model for
351 each neuron where the firing rate in successive time bins was predicted as a linear
352 combination of the monkey's own joint positions, or his partner's joint positions (Figure
353 5A; see Methods).

354 We then plotted the cross-validated model correlation of the partner joints model
355 for each neuron against that of the self joints model for giving grooming (Figure 5B) and
356 receiving grooming (Figure 5C). We observed a striking dissociation: in all brain regions,
357 neural responses of the groomer were always predicted better by the receiver's joints
358 during giving grooming in both monkeys (Figure 5D). Conversely, while receiving

359 grooming, neural responses of both monkeys were predicted better by their own joints
360 than by the joints of their partner who was grooming them (Figure 5D). This pattern
361 unfolded dynamically over time, revealing rises and falls presumably at times when the
362 animal was more closely tracking his partner (Section S6).

363 Thus, neural activity in both the groomer's and receiver's brains are strongly driven
364 by the grooming receiver's joint positions, suggesting that the monkey receiving groom
365 drives the ongoing interaction.

366

367 **Neural mirroring of joint position tuning during social interaction**

368 Social interactions require tracking our partner's intentions and movements and
369 linking them to ours. Indeed, "mirror neurons" have been reported in premotor regions
370 which have congruent tuning for self and partner movements (Rizzolatti and Craighero,
371 2004). To investigate this issue further, for each neuron, we built a model where its firing
372 rate was predicted as a linear combination of both the self joint positions and partner joint
373 positions (Figure 5E).

374 In this combined model, we calculated the correlation between the model weights
375 for self joints and partner joints. A positive correlation would imply that single neurons
376 have similar tuning for self and partner joints, as might be expected for mirror neurons. A
377 lack of correlation (i.e., zero correlation) would imply that different populations of neurons
378 keep track of self and partner joints. A negative correlation would imply that observing a
379 partner moving his joint would reduce the firing rate in neurons coding for that joint
380 movement in oneself, which could be potentially useful to avoid making self movements

381 while observing others' actions. All three possibilities are conceptually interesting, and
382 have not been studied systematically during natural social interactions in primates.

383 In all three brain regions but most prominently in PMv, we observed a negative
384 correlation on average between model weights for self and partner joints, consistent with
385 the third possibility above (Figure 5G). At the single neuron level, however, there was
386 considerable diversity, with neurons showing both significant positive and negative
387 correlations (Figure 5F; positive correlations: 3.3 % of 243 neurons in IT, 2.2% of 185 in
388 PMv, 3.3% of 61 in PFC; negative correlations: 7.4 % in IT, 9.7% in PMv, 11.5% in PFC).

389 We conclude that a subset of neurons in high-level sensory and motor regions
390 show congruent encoding of joint positions of both self and partner joints, providing a
391 neural basis for tracking the intentions of the social partner.

392

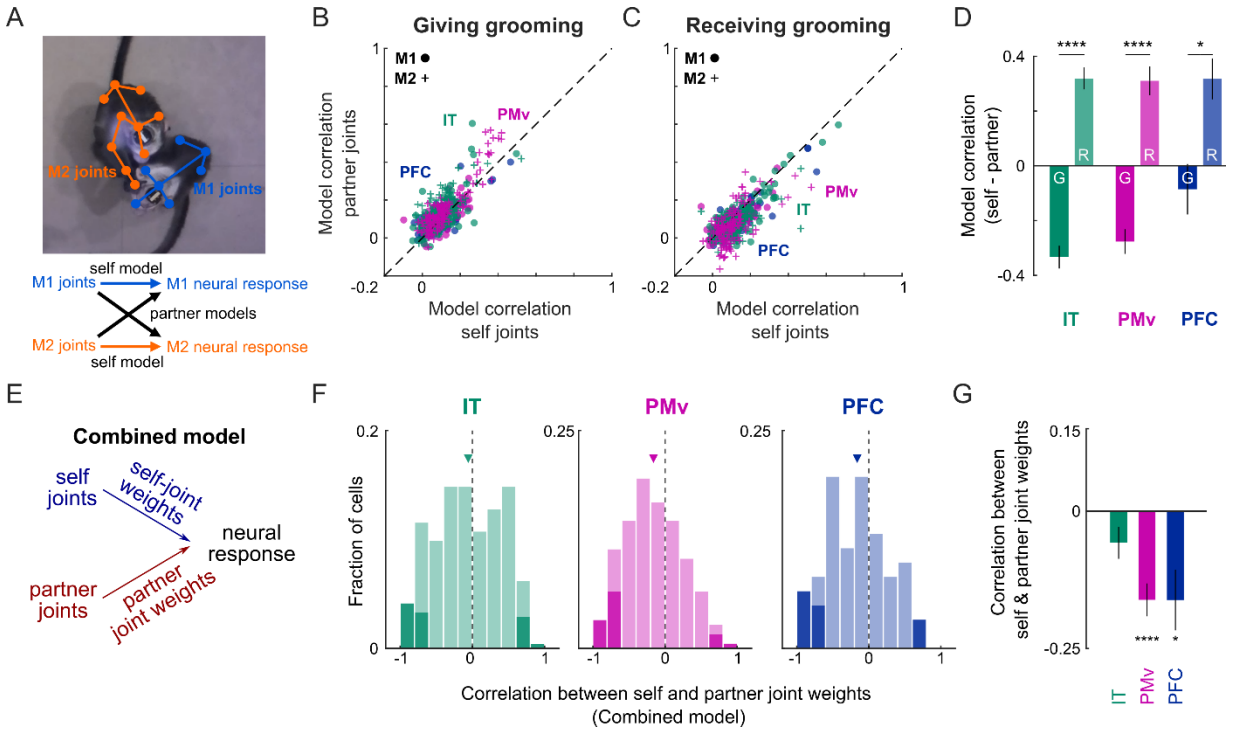

Figure 5. Neural tracking of self and partner movements during social interaction

(A) *Top:* Example screenshot from the top view of the two socially interacting monkeys, with manual joint annotations marked for M1 (*blue*) and M2 (*orange*). *Bottom:* schematic of joint models: we predicted the firing rate of each neuron in M1 and M2 using the manually annotated joint positions of M1 and M2.

(B) Cross-validated correlation between predicted and observed firing rate across time bins of the partner joint model plotted against that of the self-joint model for each neuron in IT (*green*), PMv (*purple*) and PFC (*blue*) for monkeys M1 (*dots*) and M2 (*crosses*) during the giving grooming condition. Here, the partner joint model performed better than the self joint model.

(C) Same as (B) but in the receiving grooming condition. Here, the self-joint model performed better than the partner joint model.

(D) Difference in correlation between self and partner joint model correlations (mean ± s.e.m) for IT (*green*), PMv (*purple*) and PFC (*blue*) in the giving (G) and receiving (R) grooming conditions. Asterisks indicate significance of the model correlation comparison, obtained using sign-rank test (* is $p < 0.05$, **** is $p < 0.00005$).

(E) Schematic of the combined model in which the firing rate of each neuron in successive time bins was predicted as a linear combination of self and partner joints.

(F) Histogram of correlation between self and partner joint weights across neurons in IT (left), PMv (middle) and PFC (right), with inverted triangles indicating the means. Dark bars indicate neurons with significant correlation ($p < 0.05$)

(G) Correlation (mean ± s.e.m) between the model weights for the self joints and partner joints for IT (*green*), PMv (*purple*) and PFC (*blue*). Asterisks indicate statistically significant deviations from zero, obtained using sign rank test (* is $p < 0.05$, **** is $p < 0.00005$).

421 **Interbrain coupling during social interaction**

422 Since social interactions involve close coordination with the partner, both the
423 brains might get coupled differently depending on the nature of the interaction (Figure
424 6A). To investigate this issue, in each monkey, we built a linear model to predict the
425 activity of each of his neurons using the population activity of his partner (Figure 6B, see
426 Methods).

427 In both monkeys, there was a substantial fraction of PMv/PFC neurons whose
428 activity was significantly predicted by the partner's brain activity (64% in M1, 52% in M2,
429 $p < 0.05$ for partner model correlation). To investigate whether this interbrain coupling
430 differs across grooming states, we calculated the average partner model correlation for
431 the significantly modulated M1 and M2 neurons for each type of grooming. This revealed
432 an interesting double dissociation: the groomer's brain activity was consistently predicted
433 better by the receiver compared to vice-versa (Figure 6C).

434 Since social interactions are dynamic, we wondered whether interbrain coupling
435 would unfold dynamically over the course of the social interaction. To this end, we took
436 the instantaneous correlation at each 0.05 s time bin between the predicted and observed
437 firing rates across all neurons, and smoothed this instantaneous correlation with a window
438 of 5 s which matched the slower movement timescales present in behavior. This revealed
439 a dynamic picture with larger interbrain coupling near transition points between grooming
440 states as well as within each grooming state (Figure 6D). We observed similar interbrain
441 coupling patterns for the other brain regions as well (Section S7). We also looked for but
442 did not find systematic differences in temporal delays or coherence at specific frequencies
443 as a function of grooming state (Section S8).

444 We conclude that social interactions involve dynamic interbrain coupling that is
445 driven by the receiver of grooming rather than the groomer. This finding is consistent with
446 our earlier observation that the groomer's neural activity is driven by the receiver's joints
447 (Figure 5).
448 Indeed, we observed several occasions during the social interaction where the
449 receiver adjusted his position to indicate where he wanted to be groomed, demonstrating
450 that the social interaction was indeed driven by the receiver and not the groomer (Video
451 S1).
452
453

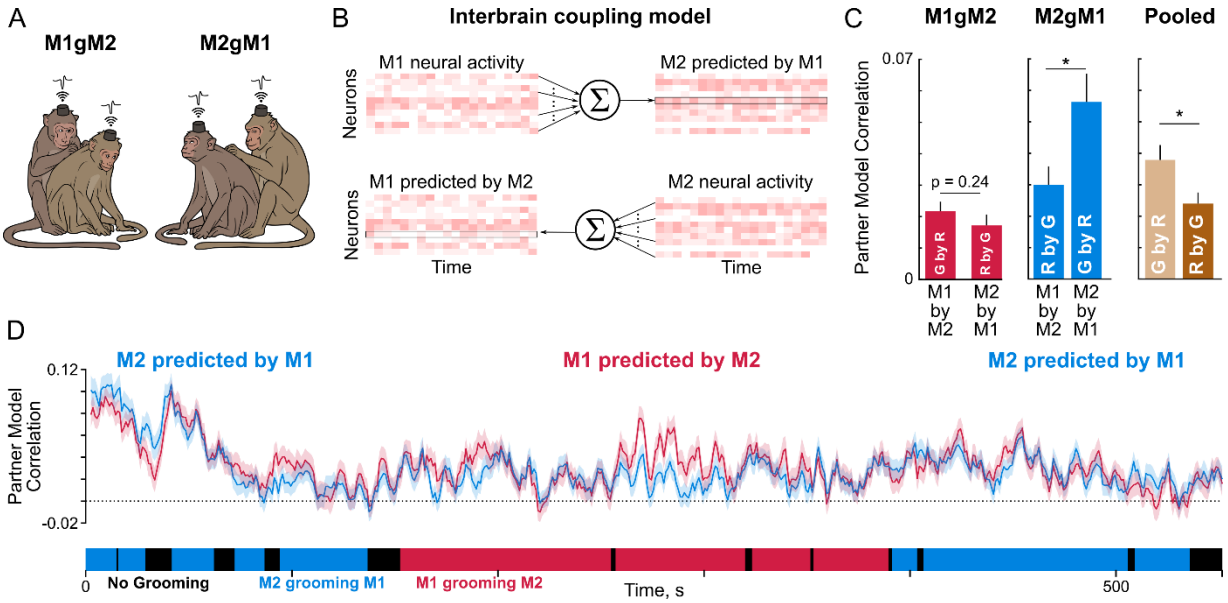

Figure 6. Interbrain coupling and its modulation by grooming state in PMv/PFC.

(A) Schematic of the two grooming states observed during social interaction: M1 grooming M2 (*left*) and M2 grooming M1 (*right*).

(B) Schematic of the interbrain coupling model. For each monkey (M1/M2), we built a model to predict the firing rate of his neurons using the PMv and PFC population neural activity of his partner, in 50 ms time bins (see Methods).

(C) Partner model correlation (mean + s.e.m) for M1 and M2 while M1 groomed M2 (*left, red bars*), while M2 groomed M1 (*middle, blue bars*), and for the data pooled for the groomer and receiver monkeys (*right, G by R* is the partner model correlation for the groomer's neurons predicted by the receiver's neurons; *R by G* is partner model correlation for the receiver monkey neurons). Asterisks indicate statistically significant comparisons (* is $p < 0.05$, rank-sum test across neurons).

(D) Time course of smoothed partner model correlation during the entire interaction (mean ± s.e.m across 50 ms time bins in each 5 s window). It can be seen that partner model correlations vary dynamically across the entire social interaction.

Convergence between behavior and multiple neural signals

In the preceding sections we have shown that, during the social interaction, brain activity in both monkeys revealed dynamically varying signals related to the grooming surplus, partner identity, partner joints, interbrain coupling and brain oscillations. Although we have reported that each signal was separately modulated by the grooming state and that each signal varied dynamically throughout the session, our analyses so far do not integrate the dynamics of these signals to interpret them in the light of the ongoing behavior. For instance, there could be specific behavioral events at which all signals show clear and interpretable modulation. Conversely, there could be times at which a neural signal attains a peak, and there is some interesting ongoing behavior at that time. To this end, we closely scrutinized the behavior of both monkeys as well as the corresponding neural signals, to find convergent and interpretable links. We summarize our observations briefly below, and refer the reader to Section S9 for details.

We noted several interesting convergences between behavior and all the neural signals. First, when M2 stopped grooming M1 (Video time = 266 s), M2 turned around and presented his back to M1, M1 huddled up against M2 and both made lip-smacking gestures and M1 began to groom M2. During this time, we found that M1 initially tracked his partner's identity (when M2 stopped groooming M1), then M2 tracked his partner's identity (when M1 began to groom M2), as evidenced by partner identity decoding. M1 closely tracked his partner's joints, while M2 tracked both his own and partner's joint movements. M1's brain activity is better predicted by M2, indicating interbrain coupling. All these neural signals point to a consistent, ongoing internal state in the two monkeys.

Likewise, when M1 was grooming M2 (Video time = 520 s), M2 started grooming M1 and M1 immediately responded by stopping his grooming. During this time, M1 was relaxed, as evidenced by high alpha power. M2 was tracking his partner's identity, as evidenced by partner decoding. Both monkeys were tracking the receiver's joints. M2's brain was predicted better by M1's brain, indicating interbrain coupling.

Finally, there were several neural events where alpha power reached a peak in each monkeys' brain. This was usually when that monkey was receiving grooming and looking up either at the roof or had his eyes closed. These observations suggest that the receiver of grooming is in a relaxed state. We also observed several moments when the alpha power attained smaller peaks while giving grooming, thus suggesting that the groomer also might be in a relaxed state while grooming his partner. This is consistent with similar observations made in the wild (Yates et al., 2022).

507 **GENERAL DISCUSSION**

508 Here we investigated the neural basis of primate social interactions by
509 simultaneous wireless brain recordings from the high-level visual and motor regions of
510 two male bonnet macaque monkeys interacting naturally without any constraints. Our
511 main findings are: (1) single neurons, primarily in IT, encoded a social favor signal
512 representing the net duration spent in giving minus receiving grooming in both monkeys,
513 providing a neural basis for grooming reciprocity; (2) neural activity in each monkey
514 tracked the grooming state as well as the partner's identity; (3) neural activity in both
515 monkeys were driven strongly by the joints of the receiver of grooming; (4) neural activity
516 in the groomer's brain was predicted better by the receiver's brain than vice-versa. These
517 findings suggest that the monkey receiving grooming directed his partner's interaction,
518 which was evident in behavior (Video S1). Below we discuss these findings in relation to
519 the existing literature.

520 A striking observation from our study is that neural activity in IT cortex of each
521 monkey tracked the relative time spent in giving versus receiving grooming (Figure 2).
522 This finding is congruent with the recent observation that IT and PFC neurons in individual
523 monkeys interacting with a partner can predict net grooming duration (Testard et al.,
524 2024). However, our study goes a step further to demonstrate a simultaneous correlation
525 between each monkeys' neural activity and his ongoing grooming surplus (Figure 2). We
526 have also shown that grooming surplus was encoded most strongly by IT compared to
527 PMv and PFC. At first glance, it is somewhat surprising that a visual region (IT) rather
528 than motor regions (PMv/PFC) should encode the grooming surplus. However, we
529 propose that this is quite reasonable considering that encoding such a signal, if encoded

530 in the motor cortex, would interfere with ongoing motor output. We also caution that it is
531 unlikely that IT would be the sole carrier of such a signal, since social interactions can
532 evoke widespread brain activation and any of these brain regions could encode social
533 favor signals (Wittmann et al., 2018; Freiwald, 2020; Deen et al., 2023).

534 Previously, in monkeys trained to play social games with a partner under artificial
535 constraints, prefrontal neurons keep track of the partner's choices, reward states and
536 strategies (Yoshida et al., 2012; Haroush and Williams, 2015; Ong et al., 2021; Chang et
537 al., 2013; Báez-Mendoza et al., 2021). Our finding that neural activity tracks key variables
538 like grooming state (Figure 3), partner identity (Figure 4) and partner's joint movements
539 (Figure 5) is congruent with these studies. However, our findings go a step further to
540 demonstrate that such tracking occurs spontaneously in natural social interactions in
541 monkeys without any extensive social training.

542 Our finding that grooming state can be decoded from neural activity in all regions
543 (Figure 3) is to be expected, since the sensory inputs and motor outputs during each
544 grooming state are likely to be quite different in nature. Perhaps what is more interesting
545 is that grooming state could be continuously decoded throughout the social interaction
546 (Figure 3F), even though sensory inputs or motor outputs were dynamically changing
547 throughout.

548 Our finding that IT neurons track partner identity during the social interaction
549 (Figure 4) is likewise expected given that they carry invariant information about objects
550 and faces (DiCarlo et al., 2012). However, our finding of robust generalization of partner
551 identity decoding from images on a screen to a real-world social interaction has not been
552 reported previously. More interestingly, we have found that partner identity decoding was

553 remarkably stable throughout, even while receiving grooming, when the monkeys were
554 often looking away from their partner. Thus, IT neurons track socially relevant stimuli even
555 when they are not directly visible.

556 We have found that neural activity in all three recorded brain regions (IT, PMv,
557 PFC) is reliably predicted by both self and the partner's joint movements (Figure 5).
558 Interestingly, in all three regions, brain activity was better predicted by the partner's joints
559 while giving grooming than while receiving grooming, and was better predicted by its own
560 joints while receiving grooming. We speculate that this could be because the receiver is
561 driving the grooming interaction by constantly adjusting his position, causing the groomer
562 to keep track of the receiver's joints. We note that all three regions are well-positioned for
563 this kind of tracking: IT could encode specific visual features of each joint, while PMv and
564 PFC are involved in motor movements and also receive projections from IT, and could
565 therefore encode both self and partner joints (Rizzolatti and Craighero, 2004).
566 Interestingly, we found neurons with both positive and negative correlations in tuning for
567 self and partner joints, which provide a neural basis for understanding the social partner's
568 intentions (Rizzolatti and Craighero, 2004). However, the prevalence of negative
569 correlations between self and partner joint tuning suggests that in social interactions, a
570 movement made by the social partner might have the overall effect of inhibiting a similar
571 movement in oneself, while facilitating reciprocating joint movements. We speculate that
572 this inhibition of joint-related activity could also provide a neural substrate for tracking
573 partner joints, since the reduced neural activity could be used to interpret the social
574 partner's actions. Taken together, our study demonstrates the spontaneous tracking of
575 partner joints during natural social interactions.

576 We have observed substantial interbrain coupling that varies dynamically
577 throughout the social interaction (Figure 6). This is consistent with previous reports of
578 interbrain coupling in bats (Zhang and Yartsev, 2019; Rose et al., 2021), mice (Kingsbury
579 et al., 2019; Zhang et al., 2025) and even humans (Stephens et al., 2010; Kinreich et al.,
580 2017). Such interbrain coupling during social interaction is presumably due to common
581 sensory and motor events experienced by the interacting individuals. However, interbrain
582 coupling between socially interacting monkeys has never been observed previously due
583 to the challenges involved in obtaining such brain recordings. Our finding that the
584 groomer's brain activity is driven by the receivers' brain activity (Figure 6) is consistent
585 with our observation that the receiver's joints drive the groomer's brain activity (Figure 5)
586 – these observations suggest that it is the receiver of grooming that drives the social
587 interaction, and not the groomer. This finding is surprising at first glance, because one
588 would expect the groomer's movements to cause sensations in the receiver. However, a
589 closer inspection of the social interactions revealed that the receiver monkey kept
590 indicating where it wished to be groomed, suggesting that it indeed drove the social
591 interaction (Video S1). Such referential gesturing has also been observed in the wild
592 (Gupta and Sinha, 2016). More broadly, our results show that interbrain coupling occurs
593 dynamically throughout the social interaction but with directionality depending on the
594 social context.
595

596 **Understanding social interactions in the wild**

597 Our study represents a first step towards studying the neural basis of primate
598 social interactions in a naturalistic setting. We have characterized brain activity during

599 only one specific dyadic social interaction, but primate social behaviors are far more
600 complex. For instance, allogrooming reciprocity could occur not just within a single
601 session but can potentially take place over multiple interactions or sometimes not at all
602 (Sinha, 1998; Adiseshan et al., 2011; Onishi et al., 2013; Gupta and Sinha, 2016; Molesti
603 and Majolo, 2017). Non-reciprocal interactions frequently occur for other reasons as well.
604 For instance, a subordinate might groom a dominant individual after an aggressive
605 interaction, and this interaction is often one-sided. Likewise, subordinates or dominant
606 individuals may initiate grooming towards another individual multiple times, but each
607 interaction may be very brief and non-reciprocal (Ram et al., 2003; Sinha et al., 2005; Xia
608 et al., 2013). We speculate that, in such cases, the social favor signal might start from a
609 non-zero (positive or negative) value and go to a baseline level after the interaction is
610 over. We also speculate that, since it could be tedious to maintain a non-zero social favor
611 signal at the neural level, social interactions would be reciprocal by default unless there
612 is some compelling reason for them not to be so.

613 Monkeys keenly observe other dyadic interactions in their social group to learn or
614 update their knowledge of social dominance in their social group (Sinha, 1998, 2017).
615 Interestingly, their behavior is predicted better by the duration rather than the frequency
616 of grooming interactions between two individuals (Sinha, 1998). This is consistent with
617 our observation that neural responses track the duration of grooming rather than the
618 number of grooming bouts (Section S2). However, an individual might make many
619 attempts to groom or solicit grooming directed at specific group members. We speculate
620 that, in this case, neural activity might keep track of the frequency of these interactions
621 as well. Indeed, we have found the number of grooming bouts also uniquely explains

neural activity (Section S2). Based on all these observations, we speculate that the social brain of an individual maintains a long-term social ledger of his own interactions with each individual in their social group, as well as a record of the prevailing hierarchy of the entire social group (Sinha, 1998, 2017).

Conclusions

In sum, our results show that important social variables, such as the ongoing social favors, grooming state, partner identity and joint movements are encoded in high-level visual and motor regions, providing a rich and dynamic neural substrate for the ongoing social interaction.

632 **METHODS**

633 All animal experiments were performed according to a protocol approved by the
634 Institutional Animal Ethics Committee of the Indian Institute of Science, Bangalore
635 (CAF/Ethics/750/2020) and by the Committee for the Purpose of Control and Supervision
636 of Experiments on Animals, Government of India (V-11011(3)/15/2020-CPCSEA-DADF).
637 Many experimental procedures are common to previously reported studies from our
638 laboratory (Ratan Murty and Arun, 2015; Jacob et al., 2021), and summarized briefly
639 below.

640

641 **Neurophysiology**

642 We implanted two adult bonnet macaque monkeys (*Macaca radiata,* M1: *Co* & M2:
643 *Di*, aged 9.5 years) with Floating Microelectrode Arrays (FMA) from Microprobes for Life
644 Science using standard neurophysiological procedures. Each FMA had 32 single-shank
645 microelectrodes arranged in a 4 x 8 grid with an inter-electrode spacing of 400 microns.
646 Monkey M1 was implanted with 4 FMAs into the central portion of the left inferior temporal
647 (IT) cortex, 2 FMAs in the left ventrolateral prefrontal cortex (PFC), and 2 FMAs in the left
648 ventral premotor cortex (PMv). Monkey M2 was implanted with 4 FMAs in the right inferior
649 temporal cortex and 4 FMAs in the right ventral premotor cortex. In both monkeys, these
650 FMAs were connected to a custom-designed titanium pedestal fixed to the skull,
651 containing headstages and wireless interface boards,. Each monkey underwent a single
652 surgery under anaesthesia using standard procedures (Ratan Murty and Arun, 2015).

653 On the day of recording, each monkey was brought into a custom chair and its
654 snout was restrained temporarily (for ~5 minutes) in order to fix the wireless logger to the

655 titanium pedestal using screws. Extracellular wideband signals were logged at 25 KHz
656 using a custom wireless logger that was synchronized to a neural data acquisition system
657 (*eCube,* White-Matter LLC). These wideband signals were high-pass filtered and
658 thresholded using a commercial software (*OfflineSorter*, Plexon Inc) to obtain multiunit
659 activity.
660
661 **Social interaction**
662 The social interaction was conducted in a naturalistic environment described
663 previously (Jacob et al., 2021). Five video cameras were positioned around the room to
664 capture the behavior of the interacting animals from multiple views, of which three
665 cameras were time-synchronized to the neural recordings by the neural data acquisition
666 system, and the other two were synchronized offline using alternative methods.
667 Both monkeys were housed together in a larger social group since birth and so
668 were already socially compatible. After including them into our study, we pair housed
669 them fully until they were implanted for brain recordings, after which they were in
670 neighbouring enclosures, separated by a metal grill as a precaution to prevent damage
671 to their brain implants due to aggressive interactions. For a few days before the brain
672 recordings, both monkeys were paired for about 30 minutes each day, to reconfirm their
673 compatibility. On the day of recording, we paired them and allowed them to interact freely
674 and naturally without any human intervention. They interacted intensively for ~11 minutes
675 while we recorded their brain activity simultaneously. After this, they stopped engaging
676 with each other and we stopped the recording.

677 After the social session, we selected one video camera feed in which most joints
678 of both monkeys were clearly visible (netcam e3v817d, top view, 30 fps; Figure 5A). We
679 used this video feed to manually mark the joint positions and used the CCTV camera
680 videos to mark the times of all relevant social behaviors such as mounting, grooming and
681 licking. We also marked the times at which each hand was used by each monkey. In
682 addition, we manually annotated the joint positions of each monkey clearly visible in each
683 frame throughout the session at 7-frame (0.233 s) intervals (joints annotated: head, neck,
684 hip, right/left shoulder, elbows, wrists, palms, side-hips, knees, ankles and feet as well as
685 the logger on the head; all annotated using NAPARI software). Joints that were not visible
686 were marked as NaN (not a number). For all further analyses, we subtracted from the (x,
687 y) position of each joint the (x, y) coordinates of the respective monkeys' wireless logger,
688 to obtain the joint position of each joint relative to the monkey's own body.
689 The total duration of the social recording was 682 seconds. We observed unusually
690 high firing in many PMv neurons of monkey M2 from 0-130 s of the session start. Since
691 this unusual high firing could potentially confound the results, we removed this period
692 from all further analyses. All results are shown with zero indicating start of analysis unless
693 specified otherwise. We obtained qualitatively similar results even upon including this
694 initial window. Similarly, we observed anomalous high-amplitude fluctuations in multi-unit
695 activity (MUA) or local field potential (LFP) from some electrodes, and therefore excluded
696 these from further analyses. All multiunit analyses are reported from 243 IT neurons (118
697 in M1, 125 in M2), 185 PMv neurons (57 in M1, 128 in M2) and 61 PFC neurons (all from
698 M1). Likewise, all LFP analyses are reported from 215 IT sites (106 in M1, 109 in M2),
699 153 PMv sites (43 in M1, 110 in M2) and 60 PFC sites (all in M1).

700 **Touchscreen tasks**

701 In order to interpret the neural activity during the social interaction as being of
702 sensory or motor origin, we trained each monkey to perform a visual task and a motor
703 task on a touchscreen attached to a juice spout, with custom-built eye tracking described
704 previously (Jacob et al., 2021).

705

706 *Visual task.* The visual task consisted of an eye calibration block and two fixation blocks.
707 In the first eye calibration block, the monkey had to initiate the task by touching a circular
708 button (4° radius) kept at (20°,0°) relative to the center of the screen within 10 s of its
709 appearance. After this, four gray circles of 0.5° radius appeared sequentially (in random
710 order) at four corners of a square 8° away from the center of the screen. Monkeys had to
711 fixate each gray circle for 0.3 s successively, after which they received a juice reward.
712 The trial was aborted if the monkey failed to fixate on the gray circle within a stipulated
713 time (0.5 s). We recorded two correct trials of the calibration block. This data was used to
714 learn a simple linear mapping between the eye tracker signal (x & y, arbitrary voltage
715 units) and the touchscreen gaze location (x, y in degrees). We used this mapping to
716 transform eye signal values in the fixation block to degrees of visual angle.

717 In the fixation blocks, the monkey had to start the trial by touching a blue button
718 (4° radius) at (28°, 0°) relative to the center of the screen. Following this, a yellow fixation
719 dot (0.1° radius) appeared at the center for 0.5 s. Upon successfully fixating for 0.3 s
720 within a fixation window (10° radius), a sequence of 8 images was presented at the center
721 of the screen, with each image appearing for 0.2 s followed by a blank screen of 0.2 s. If
722 the monkey successfully maintained fixation within a certain window and maintained

723 touch on the hold button within a certain window till the end of the trial, the trial was
724 marked correct and the monkey was rewarded with juice (~0.15-0.2 ml). Error trials were
725 repeated after a random number of other trials. Since each monkey had different patterns
726 of looking and touching, we used different hold button buffer windows (8° for M1, 2° for
727 M2) and fixation windows (10° for face images for M1 and M2, 22° for body images for
728 M1 and M2). Although the fixation window was kept relatively large, post-hoc analyses
729 revealed that both monkeys eye positions were closely centered on the screen center
730 throughout the trial (standard deviation of eye position during a trial: 0.65° for horizontal
731 and 0.51° for vertical for M1, and 0.78° for horizontal and 0.70° for vertical for M2,
732 averaged across trials; mean jitter in eye position across trials: 0.1° for horizontal and
733 0.22° for vertical for M1, and 0.2° for horizontal and 0.13° for vertical for M2).

734 The stimuli in the fixation block comprised photographs of 3 monkeys from the
735 facility - M1 (*Co*), M2 (*Di*) & M3 (*Tu*) – that were photographed from different viewpoints.
736 Monkey M3 was also group housed with the two monkeys before they were implanted.
737 We selected five roughly matched views of each monkeys' face (left, left-oblique, front,
738 right and right-oblique), and five roughly matched views of each monkeys' body in various
739 poses (walking/sitting). Thus, there were 30 stimuli (3 monkeys x 5 face views + 3
740 monkeys x 5 body views). All the face images were scaled to measure 13.6° along the
741 longest dimension, and body images were scaled to measure 43.8° along the longest
742 dimension, to roughly match the size in real-world interactions. To avoid any potential
743 neural response adaptation, successive images in a trial did not contain the same view
744 or same monkey identity. Since image sizes were different for face and body images, they
745 were presented in two separate blocks. Each monkey performed 60 correct trials of the

746 fixation block, yielding 16 repetitions of each image which we used for subsequent
747 analyses.
748
749 *Motor task.* The motor task consisted of a calibration block which was the same as before,
750 and a reach block. Each monkey performed the same task twice, once using his left hand
751 and once with his right hand. We made monkeys switch their hand by fixing a metal grill
752 on the left/right side of the juice spout that made it inconvenient to use the left/right hand
753 to perform the task. Both monkeys were trained extensively to use the right hand for many
754 other tasks, but adapted readily to use the left hand when the grill was placed to block
755 access to their right hand.
756 In the reach block, each trial started with a green button that appeared 15° from
757 the center on the left or right. After touching the button for 0.3 s, a second button appeared
758 at one of four possible locations (up/down/left/right) equidistant (13°) from the center. The
759 monkey had to touch the target button as soon as possible, and he received juice for
760 correctly touching the button. Each monkey had to perform 64 correct trials (4 reach
761 directions x 16 repeats). Error trials were repeated after a random number of other trials.
762 For each monkey, we recorded separate sessions on the same day for the left and right
763 motor tasks.
764
765 **Correlation with grooming surplus (Figure 2)**
766 To compute the correlation between neural activity and the grooming surplus, for
767 each time windows of 30 s each throughout the social interaction, we calculated the
768 cumulative time spent by each monkey in grooming its partner minus the cumulative time

769 spent receiving grooming. Likewise, we calculated the average firing rate of each neuron
770 in these time windows. The correlation reported in Figure 2 is the Pearson's correlation
771 coefficient between the grooming surplus and the average firing rate across neurons
772 (Figure 2C), or between grooming surplus and the firing rate of each neuron (Figure 2D-
773 E).
774
775 **Grooming state decoding (Figure 3)**
776 To investigate if population neural activity can be used to decode the current
777 grooming state, we used a linear decoding analysis. We calculated the neural activity in
778 successive 0.5 s bins across all neurons to form a vector of neural activations, and for
779 each such bin, we assigned a 3-way label based on the corresponding grooming state in
780 that bin (giving grooming, receiving grooming or no grooming). Bins containing a transition
781 from one grooming state to another were excluded. To train the decoder, we first projected
782 the multidimensional vectors corresponding to all bins into a low-dimensional space using
783 principal component analysis by selecting principal components to capture 90% of the
784 variance. We then trained the classifier using 5-fold cross-validation (*classify* function,
785 MATLAB): in each training fold, we trained the classifier on 80% of the bins, and tested it
786 on the held-out 20% of the bins. We concatenated the decoding accuracy for each held-
787 out 20% of the data to obtain the cross-validated decoding label for all bins. By comparing
788 this cross-validated decoding label with the actual label for each bin, we obtained a binary
789 vector containing 0s for bins when the decoder was wrong and 1s for bins when the
790 decoder was correct. Grooming decoding accuracy was calculated as the mean and
791 standard error of this vector across bins.

792

793 **Partner identity decoding (Figure 4)**

794 To decode the identity of the social partner, we first trained a 3-way linear decoder
795 (using the same approach as the grooming state decoding) on the population neural
796 activity from IT in the visual task elicited by the faces of M1, M2 and M3 during a 0-0.2 s
797 window after image onset. The cross-validated decoding accuracy on the fixation task is
798 shown using the red lines in Figure 4B-C.

799 To investigate whether this decoder, trained on the responses to face images on
800 the touchscreen, would correctly decode the social partner's identity during the social
801 interaction, we calculated the population neural response vector during the social session
802 in successive 0.5 s bins, centred each vector by subtracting the average firing rate of the
803 corresponding grooming state and projected them into the principal components in the
804 touchscreen task and obtained the predicted labels from the classifier. We excluded bins
805 with transitions between the grooming bouts since those labels are ambiguous. The
806 decoder was deemed correct in that bin and scored as 1 if the decoded identity was that
807 of the social partner (i.e. for M1, social partner would be M2, and vice-versa) and scored
808 as 0 if the predicted label was incorrect. Partner decoding accuracy was calculated as the
809 mean and standard error of this vector across bins.

810

811 **Neural tracking of self & partner joint positions (Figure 5A-D)**

812 To investigate whether single neurons were tracking the joint positions of the
813 monkeys' own joints (self) and that of its social partner, we first selected a subset of joints
814 for further analysis. Of the 20 manually annotated joints, we found that upper body joints

such as head, neck & shoulders (left & right) of both monkeys were visible in 79.3% of the frames, whereas other joints such as ankle and knee were frequently occluded or not clearly visible. We therefore selected these four joints (head, neck, left & right shoulder) for further analyses (Figure 5A). Including more joints into the model resulted in less data to fit the model, but yielded qualitatively similar results. Of the 2366 camera frames available from the manual annotations, we took 1876 camera frames with all these joints visible in both monkeys for further analyses.

For each neuron in each monkey, we calculated the firing rate in successive bins of the same width as the camera frame intervals centered on the camera frame times, and asked whether the firing rates across all these bins can be predicted as a weighted sum of the joint positions of itself, or its social partner. This amounted to solving a set of linear equations of the form $\boldsymbol{y} = \boldsymbol{X}\boldsymbol{b}$, where $\boldsymbol{y}$ is an 1876 x 1 vector of firing rates of the neuron in each time bin across all three grooming states, $\boldsymbol{X}$ is a 1876 x 9 matrix containing the (x, y) coordinates of the head, neck, left and right shoulders and a constant, and $\boldsymbol{b}$ contains the weights of the linear summation. To evaluate this model, we used 10-fold cross-validation: we trained the model on 90% of the bins, and tested on the held-out 10% of the bins repeatedly to obtain a cross-validated prediction for all bins. Model performance was taken as the correlation coefficient between the predicted model output obtained in this manner with the observed firing rate, performed across bins of each grooming state (giving & receiving grooming). In this manner, we obtained the self joint model correlation (i.e. how well the neural response was predicted by the monkey's own joints) and the partner joint model correlation (i.e. how well the neural response was

837 predicted by the social partner's joints) for each grooming state, which is shown in Figure
838 5B.

839 We note that these correlations are relatively low on average because the firing
840 rates are based on discretizing the response into small time bins without the benefit of
841 collecting multiple trials. We observed similar levels of correlation when we fit single trial
842 firing rates in the visual task as a weighted sum of convolutional neural network (VGG-
843 16) activations, but we found much higher correlations upon fitting the same model to
844 firing rates averaged across trials (data not shown).

845

846 **Neural mirror tuning for self & partner joints (Figure 5E-F)**

847 To investigate whether neurons show similar tuning for self and partner joints, we
848 created a combined model for each neuron in each monkey, where the neural response
849 is taken as a weighted sum of the joint positions of its own joints as well as its partner's
850 joints (Figure 5E). The resulting model weights capture the tuning to both self joints (n =
851 8 weights) and partner joints (n = 8 weights) in the same model. To calculate model
852 weights, we fit the model on firing rates across all bins, and calculated the correlation
853 between the weights of the self joints and the partner's joints. A positive correlation implies
854 that a neuron that increases its firing for the monkey's own joints also increases its firing
855 when the partner's joints move in the same way – in other words, this is the classic mirror
856 neuron response. By contrast, a negative correlation means that the neuron that shows
857 increases in firing for its own joints will decrease its firing when the partners joints make
858 a similar movement – such activity would avoid direct production of movement upon

observing one's partner, yet enable understanding of the partner's movements. These correlations are reported in Figure 5F-G.

Interbrain coupling (Figure 6)

To investigate interbrain coupling, we asked whether the firing rate of each neuron in successive 0.05 s bins could be predicted as a weighted sum of the firing rates of neurons in the partner's brain. In other words, we solved a linear regression of the form $\boldsymbol{y} = \boldsymbol{X}\boldsymbol{b}$, where $\boldsymbol{y}$ is a 11,044 x 1 vector of firing rates of the neuron, $\boldsymbol{X}$ is a 11,044 x (n+1) matrix containing the firing rates of all *n* neurons in the partner monkey along with a constant term (set to 1), and $\boldsymbol{b}$ is a (n+1) x 1 weight vector that captures the contribution of each partner monkey neuron. To evaluate this model, we used a leave-one-out cross-validation: for each bin, we trained the model on all other bins and calculated the predicted firing rate in that bin. We built separate models for IT separately & PMv/PFC. Model performance for each neuron was evaluated as the correlation coefficient between the predicted firing rate obtained in this manner and the observed firing rate across all bins of the respective grooming state. To elucidate the time course of this partner model correlation, we computed the instantaneous correlation at each time bin across all neurons. Further, we smoothened the data by taking the average correlations in a 5 s moving window with a step size of 1s, so that we can capture the dynamics in a reasonable window. This model correlation (mean ± sem) is reported in Figure 6D).

REFERENCES

Adiseshan A, Adiseshan T, Isbell LA (2011) Affiliative relationships and reciprocity among adult male bonnet macaques (Macaca radiata) at Arunachala Hill, India. Am J Primatol 73:1107–1113.

Báez-Mendoza R, Mastrobattista EP, Wang AJ, Williams ZM (2021) Social agent identity cells in the prefrontal cortex of interacting groups of primates. Science 374:eabb4149 Available at: http://www.ncbi.nlm.nih.gov/pubmed/34672743.

Berger M, Agha NS, Gail A (2020) Wireless recording from unrestrained monkeys reveals motor goal encoding beyond immediate reach in frontoparietal cortex. eLife 9:e51322.

Chang SWC, Gariépy JF, Platt ML (2013) Neuronal reference frames for social decisions in primate frontal cortex. Nat Neurosci 16:243–250.

Cisek P, Green AM (2024) Toward a neuroscience of natural behavior. Curr Opin Neurobiol 86:102859.

Deen B, Schwiedrzik CM, Sliwa J, Freiwald WA (2023) Specialized Networks for Social Cognition in the Primate Brain. Annu Rev Neurosci 46:381–401.

DiCarlo JJ, Zoccolan D, Rust NC (2012) How Does the Brain Solve Visual Object Recognition? Neuron 73:415–434 Available at: http://dx.doi.org/10.1016/j.neuron.2012.01.010%5Cnpapers3://publication/doi/10.1016/j.neuron.2012.01.010.

Fan S, Dal Monte O, Chang SWC (2021) Levels of naturalism in social neuroscience research. iScience 24:102702 Available at: https://linkinghub.elsevier.com/retrieve/pii/S2589004221006702 [Accessed October 12, 2025].

Franch M, Yellapantula S, Parajuli A, Kharas N, Wright A, Aazhang B, Dragoi V (2024) Visuo-frontal interactions during social learning in freely moving macaques. Nature:1–8 Available at: https://www.nature.com/articles/s41586-024-07084-x [Accessed February 15, 2024].

Freiwald WA (2020) Social interaction networks in the primate brain. Curr Opin Neurobiol 65:49–58.

Fujii N, Hihara S, Iriki A (2007) Dynamic Social Adaptation of Motion-Related Neurons in Primate Parietal Cortex Lu B, ed. PLoS ONE 2:e397 Available at: https://dx.plos.org/10.1371/journal.pone.0000397 [Accessed September 4, 2024].

Fujii N, Hihara S, Nagasaka Y, Iriki A (2009) Social state representation in prefrontal cortex. Soc Neurosci 4:73–84 Available at: http://www.tandfonline.com/doi/abs/10.1080/17470910802046230 [Accessed September 4, 2024].

Gilbert KM, Cléry JC, Gati JS, Hori Y, Johnston KD, Mashkovtsev A, Selvanayagam J, Zeman P, Menon RS, Schaeffer DJ, Everling S (2021) Simultaneous functional MRI of two awake marmosets. Nat Commun 12:6608 Available at: https://www.nature.com/articles/s41467-021-26976-4 [Accessed October 15, 2025].

Gupta S, Sinha A (2016) Not here, there! Possible referential gesturing during allogrooming by wild bonnet macaques, Macaca radiata. Anim Cogn 19:1243–1248.

Hansmeyer L, Yurt P, Agha N, Trunk A, Berger M, Calapai A, Treue S, Gail A (2023) Home-Enclosure-Based Behavioral and Wireless Neural Recording Setup for Unrestrained Rhesus Macaques. eneuro 10:ENEURO.0285-22.2022 Available at: https://www.eneuro.org/lookup/doi/10.1523/ENEURO.0285-22.2022 [Accessed October 9, 2025].

Haroush K, Williams ZM (2015) Neuronal Prediction of Opponent's Behavior during Cooperative Social Interchange in Primates. Cell 160:1233–1245 Available at: https://linkinghub.elsevier.com/retrieve/pii/S0092867415001233 [Accessed October 16, 2025].

Jacob G, Katti H, Cherian T, Das J, Zhivago KA, Arun SP (2021) A naturalistic environment to study visual cognition in unrestrained monkeys. eLife 10:1–30.

Kingsbury L, Huang S, Wang J, Gu K, Golshani P, Wu YE, Hong W (2019) Correlated Neural Activity and Encoding of Behavior across Brains of Socially Interacting Animals. Cell 178:429-446.e16 Available at: https://linkinghub.elsevier.com/retrieve/pii/S0092867419305501 [Accessed October 5, 2025].

Kinreich S, Djalovski A, Kraus L, Louzoun Y, Feldman R (2017) Brain-to-Brain Synchrony during Naturalistic Social Interactions. Sci Rep 7:17060 Available at: https://www.nature.com/articles/s41598-017-17339-5 [Accessed October 9, 2025].

McMahon E, Isik L (2023) Seeing social interactions. Trends Cogn Sci 27:1165–1179.

Molesti S, Majolo B (2017) Evidence of direct reciprocity, but not of indirect and generalized reciprocity, in the grooming exchanges of wild Barbary macaques (Macaca sylvanus). Am J Primatol 79.

Morin EL, Hadj-Bouziane F, Stokes M, Ungerleider LG, Bell AH (2015) Hierarchical Encoding of Social Cues in Primate Inferior Temporal Cortex. Cereb Cortex N Y N 1991 25:3036–3045 Available at: http://www.ncbi.nlm.nih.gov/pubmed/24836688 [Accessed November 20, 2017].

Ong WS, Madlon-Kay S, Platt ML (2021) Neuronal correlates of strategic cooperation in monkeys. Nat Neurosci 24:116–128 Available at: https://www.nature.com/articles/s41593-020-00746-9 [Accessed October 16, 2025].

Onishi K, Yamada K, Nakamichi M (2013) Grooming-related feeding motivates macaques to groom and affects grooming reciprocity and episode duration in Japanese macaques (Macaca fuscata). Behav Processes 92:125–130.

Parodi F, Kording KP, Platt ML (2025) Primate neuroethology: a new synthesis. Trends Cogn Sci:S1364661325002414 Available at: https://linkinghub.elsevier.com/retrieve/pii/S1364661325002414 [Accessed October 9, 2025].

Ram S, Venkatachalam S, Sinha A (2003) Changing social strategies of wild female bonnet macaques during natural foraging and on provisioning. Curr Sci 84:780–790 Available at: http://eprints.nias.res.in/1/ [Accessed March 11, 2026].

Ratan Murty NA, Arun SP (2015) Dynamics of 3D view invariance in monkey inferotemporal cortex. J Neurophysiol 113:2180–2194 Available at: http://www.ncbi.nlm.nih.gov/pubmed/25609108.

Rizzolatti G, Craighero L (2004) The mirror-neuron system. Annu Rev Neurosci 27:169–192.

Rose MC, Styr B, Schmid TA, Elie JE, Yartsev MM (2021) Cortical representation of group social communication in bats. Science 374:eaba9584 Available at: https://www.science.org/doi/10.1126/science.aba9584 [Accessed October 15, 2025].

Roy S, Wang X (2012) Wireless multi-channel single unit recording in freely moving and vocalizing primates. J Neurosci Methods 203:28–40.

Schwarz DA, Lebedev MA, Hanson TL, Dimitrov DF, Lehew G, Meloy J, Rajangam S, Subramanian V, Ifft PJ, Li Z, Ramakrishnan A, Tate A, Zhuang KZ, Nicolelis MAL (2014) Chronic, wireless recordings of large-scale brain activity in freely moving rhesus monkeys. Nat Methods 11:670–676 Available at: https://www.nature.com/articles/nmeth.2936 [Accessed October 15, 2025].

Shepherd SV, Freiwald WA (2018) Functional Networks for Social Communication in the Macaque Monkey. Neuron 99:413-420.e3 Available at: https://linkinghub.elsevier.com/retrieve/pii/S0896627318304951 [Accessed October 7, 2025].

Sinha A (1998) Knowledge acquired and decisions made: triadic interactions during allogrooming in wild bonnet macaques, Macaca radiata. Philos Trans R Soc Lond B Biol Sci 353:619–631.

Sinha A (2017) Scio Ergo Sum: Knowledge of the Self in a Nonhuman Primate. J Indian Inst Sci 97:567–582 Available at: https://journal.iisc.ac.in/index.php/iisc/article/view/4700 [Accessed March 11, 2026].

Sinha A, Mukhopadhyay K, Datta-Roy A (2005) Ecology proposes, behaviour disposes: Ecological variability in social organization and male behavioural strategies among wild bonnet macaques. Anim Behav.

Sliwa J, Freiwald WA (2017) A dedicated network for social interaction processing in the primate brain. Science 356:745–749 Available at: https://www.science.org/doi/10.1126/science.aam6383 [Accessed October 7, 2025].

Stephens GJ, Silbert LJ, Hasson U (2010) Speaker–listener neural coupling underlies successful communication. Proc Natl Acad Sci 107:14425–14430 Available at: https://pnas.org/doi/full/10.1073/pnas.1008662107 [Accessed October 9, 2025].

Testard C, Tremblay S, Parodi F, DiTullio RW, Acevedo-Ithier A, Gardiner KL, Kording K, Platt ML (2024) Neural signatures of natural behaviour in socializing macaques. Nature 628:381–390 Available at: https://www.nature.com/articles/s41586-024-07178-6 [Accessed October 7, 2025].

Testard C, Tremblay S, Platt M (2021) From the field to the lab and back: neuroethology of primate social behavior. Curr Opin Neurobiol 68:76–83 Available at: https://linkinghub.elsevier.com/retrieve/pii/S0959438821000076 [Accessed October 16, 2025].

Tseng P-H, Rajangam S, Lehew G, Lebedev MA, Nicolelis MAL (2018) Interbrain cortical synchronization encodes multiple aspects of social interactions in monkey pairs. Sci Rep 8:4699 Available at: https://www.nature.com/articles/s41598-018-22679-x [Accessed October 9, 2025].

Wittmann MK, Lockwood PL, Rushworth MFS (2018) Neural Mechanisms of Social Cognition in Primates. Annu Rev Neurosci 41:99–118 Available at: https://www.annualreviews.org/doi/10.1146/annurev-neuro-080317-061450 [Accessed October 7, 2025].

Xia D-P, Li J-H, Garber PA, Matheson MD, Sun B-H, Zhu Y (2013) Grooming reciprocity in male Tibetan macaques. Am J Primatol 75:1009–1020.

Yates K, Stanley CR, Bettridge CM (2022) The effects of allogrooming and social network position on behavioural indicators of stress in female lion-tailed macaques (Macaca silenus). Behav Processes 202:104740.

Yoshida K, Saito N, Iriki A, Isoda M (2012) Social error monitoring in macaque frontal cortex. Nat Neurosci 15:1307–1312 Available at: https://www.nature.com/articles/nn.3180 [Accessed October 15, 2025].

Zhang W, Yartsev MM (2019) Correlated Neural Activity across the Brains of Socially Interacting Bats. Cell 178:413-428.e22 Available at: https://linkinghub.elsevier.com/retrieve/pii/S0092867419305513 [Accessed October 5, 2025].

Zhang X, Phi N, Li Q, Gorzek R, Zwingenberger N, Huang S, Zhou JL, Kingsbury L, Raam T, Wu YE, Wei D, Kao JC, Hong W (2025) Inter-brain neural dynamics in biological and artificial intelligence systems. Nature 645:991–1001 Available at: https://www.nature.com/articles/s41586-025-09196-4 [Accessed October 9, 2025].

ACKNOWLEDGEMENTS

We thank Anindya Sinha for valuable insights into primate social interactions, Dr. Sebastian Chandu for assistance with neurosurgeries, Dr. Sumedh Shastry for assistance with physiology during neurosurgeries and post-surgical care, Dr. Sumedh Shastry & Mr. V. Ramesh for primate facility management and animal care, Ravi & Ashok for animal care and Dharshana Raj & Vera Rao for assistance with manual annotation of joint positions.

FUNDING

This research was supported by the DBT/Wellcome Trust India Alliance Senior Fellowship (Grant# IA/S/17/1/503081), Indian Institute of Science internal grants, a Google Asia Pacific research grant, and an intramural grant from Pratiksha Trusts Initiatives (all to SPA).

We also gratefully acknowledge the following fellowship support from the Government of India: Simon, S: Ministry of Education (MoE); Bhadra, D: Ministry of Education (MoE); Saha, S: Prime Ministers' Research Fellowship (PMRF ID: 0200402) and Ministry of Education (MoE); Munda, S: CSIR Fellowship (ID: 35100868); Das, J: UGC Fellowship (816/CSIR-UGC NET).

DATA AVAILABILITY

All data and code required to reproduce the results are publicly available at https://osf.io/tu5ed

SUPPLEMENTARY MATERIAL

for

Dynamic encoding of social variables in simultaneous brain recordings of socially interacting monkeys

CONTENTS

- **SECTION S1. COMPARISON OF SOCIAL & TOUCHSCREEN TASKS**
- **SECTION S2. ENCODING OF GROOMING SURPLUS VS OTHER SIGNALS**
- **SECTION S3. SPIKE & LFP POWER SPECTRA ACROSS GROOMING TYPE**
- **SECTION S4. GROOMING DECODING ACROSS TRANSITIONS**
- **SECTION S5. DYNAMICS OF PARTNER & HAND DECODING**
- **SECTION S6. ADDITIONAL ANALYSIS OF SELF & PARTNER JOINT MODELS**
- **SECTION S7. INTERBRAIN COUPLING ACROSS BRAIN REGIONS**
- **SECTION S8. INTERBRAIN CROSS-CORRELATION & COHERENCE**
- **SECTION S9. CONVERGENCE BETWEEN BEHAVIOR AND NEURAL SIGNALS**

SECTION S1. NEURAL RESPONSES DURING SOCIAL & TOUCHSCREEN TASKS

We have found that both IT & PMv neurons show elevated firing rates while giving compared to receiving grooming (Figure 3C). This could be due to increased sensory inputs and motor movements during giving compared to receiving grooming. To investigate this possibility, we compared neural responses in giving vs receiving grooming with the responses of these neurons during a visual task and a motor task performed on a touchscreen (see Methods; Figure S1A).

Responses of visual & non-visual neurons in IT while giving & receiving grooming

We hypothesized that, if there is greater sensory input while giving grooming, IT neurons that are visually responsive in a fixation task on the touchscreen should also show stronger modulation while giving vs receiving grooming. We therefore manually categorized each IT neuron in the visual task as visual or non-visual based on whether it showed a clear visual response to at least one image. We then calculated the average response of the visual and non-visual neurons during a response period (0.05-0.2 s after image onset) and a baseline period (-0.05 to 0.05 s relative to image onset). As expected, by definition, we observed a strong response modulation in the visual neurons compared to the non-visual neurons (Figure S1B). Next we compared the responses of these visual and non-visual neurons during the giving & receiving grooming bins of the social interaction. Interestingly, the neurons that show strong response modulation to visual images, also showed a strong response modulation to giving compared to receiving grooming (Figure S1F). Even the non-visual neurons in IT also showed a significantly larger response during giving compared to receiving grooming, although this difference was considerably smaller compared to the visual neurons (Figure S1F; average of absolute response difference, abs(giving – receiving grooming): 1.68 ± 0.16 spikes/s for visual neurons, 1.03 ± 0.22 spikes/s for non-visual neurons, $p < 0.05$, ranksum test). These findings suggest that there is greater visual input during giving compared to receiving grooming. However, this analysis is not entirely conclusive since there are other signals in IT cortex during the social interaction that are not entirely sensory, as evidenced by the correlation with grooming surplus.

Responses of motor & non-motor neurons while giving & receive grooming

Next we hypothesized that, since there are greater motor movements during giving compared to receiving grooming, PMv neurons that are modulated by hand movements on touchscreen motor tasks should also show greater modulation for giving grooming. To this end, we manually categorized each PMv neuron in the motor task as being modulated by the movement and calculated their average response around a window relative to onset of response (0 to 0.3 s for the left hand, -0.5 to 0 s for right hand) compared to a baseline period (-0.35 to 0 s relative to sample onset).

This revealed a clear modulation in the motor task (Figure S1C-D), which is expected by definition. Upon comparing the responses of these two groups of neurons in the social session during giving and receiving grooming, we found that the motor neurons in PMv showed a clear response modulation (Figure S1G). This modulation was present strongly even in the non-motor neurons (Figure S1G), suggesting that the PMv neurons that were deemed non-motor on the touchscreen task based on only hand movements

are presumably modulated by movements of other limbs in the social task. Nonetheless, the response difference in the motor neurons was larger than in the non-motor neurons (Figure S1G; average absolute response difference, abs(giving – receiving grooming): 4.35 ± 0.48 spikes/s for motor neurons, 0.99 ± 0.12 spikes/s for non-motor neurons, $p < 0.00005$, rank-sum test). These findings suggest that there is greater motor modulation during giving compared to receiving grooming. However, this analysis is not entirely conclusive since there are other signals in PMv cortex during the social interaction that are not entirely of motor origin, such as the correlation with grooming surplus.

We observed no clear pattern in PFC neurons – if anything, the non-motor neurons in PFC showed a larger response during receiving compared to giving grooming (Figure S1D, Figure S1H).

In sum, we conclude that the increased firing rates in IT & PMv during giving compared to receiving grooming are likely due to increased sensory inputs and motor outputs while grooming.

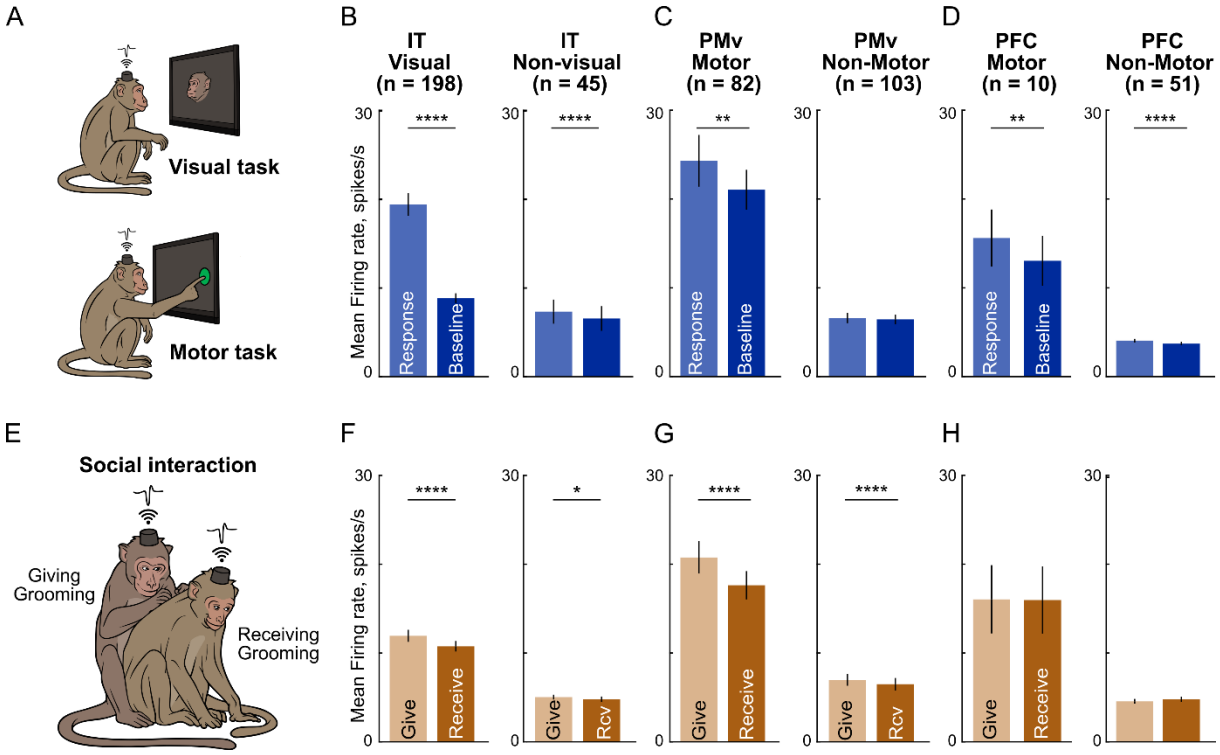

Figure S1. Visual & motor modulation during touchscreen and social tasks

(A) *Top:* Schematic of the visual task performed by each monkey separately on the touchscreen, where it had to fixate on a series of images presented visually.
Bottom: Schematic of the motor task performed by each monkey separately on the touchscreen, where it had to touch targets appearing at four possible locations on the screen.

(B) *Left:* Average firing rate of all visually responsive neurons in IT pooled across both monkeys during the image presentation period (0.05-0.2 s after image onset) and during the baseline period (-0.05 to 0.05 s relative to image onset). Asterisks represent statistical significance (* is $p < 0.05$, ** is $p < 0.005$, etc.; sign-rank test across neurons)
Right: same plot for IT neurons classified as not visually responsive.

(C) *Left:* Average firing rate of all motor-modulated neurons of PMv pooled across both monkeys aligned to the motor response and during the baseline period.
Right: same plot for PMv neurons classified as non-motor.

(D) Same as (C) but for motor & non-motor PFC neurons.

(E) Schematic of social session, depicting M1 grooming M2.

(F) Average firing rate for the visual (*left*) & non-visual (*right*) neurons in IT during giving and receiving grooming bouts.

(G) Same as (F) but for motor & non-motor neurons in PMv.

(H) Same as (G) but for motor & non-motor neurons of PFC.

SECTION S2. ENCODING OF GROOMING SURPLUS VS OTHER SIGNALS

We have found that the average firing rate of IT neurons in each monkey closely tracks the grooming surplus signal (Figure 2). However, this correlation could arise from a simple overall level difference in firing rates between giving and receiving grooming. Likewise, monkeys might count the total number of giving versus receiving grooming bouts instead of keeping track of the overall duration. More generally, the correlation we have observed between neural responses and the grooming surplus signal could be alternatively explained by other factors that also vary in other ways during this period.

To this end, we created a number of variables that could covary with the average firing rate, as listed below. These signals are shown for each monkey in Figure S2A.

1) Grooming Surplus Time (GST), which is the main grooming surplus signal, defined as the total amount of time of giving grooming minus the total time of receiving grooming.
2) Cumulative Giving Grooming Time (CGGT), defined as the cumulative time spent in giving grooming to the partner.
3) Cumulative Receiving Grooming Time (CRGT), defined as the cumulative time spent in receiving grooming from the partner. Note that GST = CGGT – CRGT.
4) Cumulative Giving Grooming Number (CGGN), defined as the total number of bouts spent in giving grooming. Our rationale was that monkeys might keep track of the number of bouts instead of the cumulative time spent.
5) Cumulative Receiving Grooming Number (CRGN), defined as the total number of bouts spent in receiving grooming.
6) Cumulative Grooming Surplus Number (GSN), defined as the cumulative number of bouts spent giving grooming minus receiving grooming. Note that GSN = CGGN – CRGN.
7) Is Giving Grooming (IGG), which is a binary signal (0/1) indicating if the monkey is grooming the partner
8) Is Receiving Grooming (IRG), which is a binary signal (0/1) indicating if the monkey is receiving grooming from his partner
9) Within Bout Cumulative Giving Grooming Time (WBCGGT), which tracks the cumulative time spent in grooming the partner within each bout.
10) Within Bout Cumulative Receiving Grooming Time (WBCRGT), which tracks the cumulative time spent in receiving grooming within each bout.
11) Within Bout Grooming Time (WBGT), which tracks the elapsed time in a bout regardless of giving or receiving grooming.

Correlation of each grooming signal with neural responses

We calculated each of these signals after smoothing the data with a 30 s boxcar window to capture the slowly varying nature of the signals (varying this choice yielded qualitatively similar results). For each neuron, we calculated the correlation between the firing rate and each variable across time, and averaged this across neurons to obtain an average correlation for a given brain region.

The resulting correlations are shown in Figure S2B for IT neurons. We find that grooming surplus time (GST) has the highest correlation, along with Is Giving Grooming (IGG; Figure S2B). Note that Is Receiving Grooming (IRG), being negatively correlated

with IGG, has a negative correlation with the neural firing of IT neurons (Figure S2B). A number of other signals were also significantly correlated with the average neural response in IT.

We obtained a different pattern of encoding in PMv neurons: here, Is Giving Grooming (IGG) had the highest correlation compared to all other factors (Figure S2C). This is expected since PMv neurons show larger firing rates during giving grooming (Figure S1G), since grooming involves motor movements. Finally, PFC neurons showed relatively lower correlations (Figure S2D) compared to PMv and PFC, presumably because of the smaller number of cells sampled, that too only in one monkey.

Partial correlation of each grooming signal with neural responses

To confirm that the correlation of a given factor with the average firing rate is not explained by other factors, we performed a partial correlation analysis, where we calculated the correlation of the average firing rate of each neuron with a given factor after regressing out the possible contribution of all other factors. Since some signals are a combination of two other signals (e.g. GST = CGGT – CGRT), we included only two of these signals into the partial correlation analyses. In the resulting analyses, a significant partial correlation of a given factor implies that it has a unique correlation with the neural response even after considering all other grooming variables.

The resulting plots are shown in Figure S2E-G. For IT neurons, we found that grooming surplus time (GST) had the highest partial correlation that was significantly different from all other grooming variables (Figure S2E). However, a number of other factors had a significant partial correlation with IT neural responses as well.

For PMv neurons, we find that IGG had the largest partial correlation with neural responses (Figure S2F), with a few other variables continuing to have a significant but smaller contribution. Finally, PFC neurons showed no significant partial correlation with any variables – however this could be due to the smaller sample of PFC neurons, that too only in one monkey.

In sum, we conclude that the grooming surplus time is encoded strongly by IT neurons along with several other grooming-relevant variables, which could form the neural basis of grooming reciprocity.

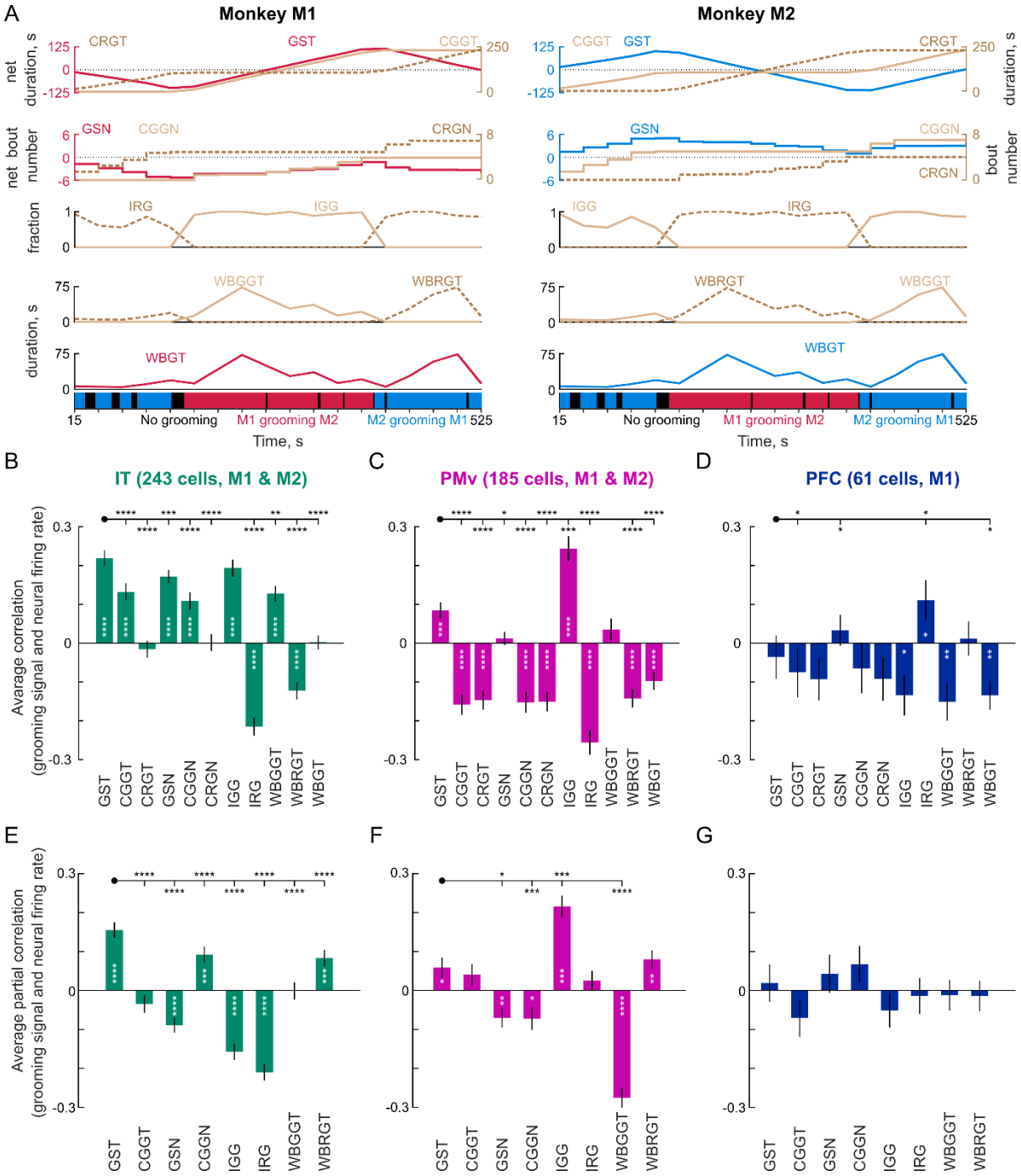

Figure S2. Encoding of grooming variables in each brain region

(A) Time course of grooming-related variables for monkey M1 (*left*) and M2 (*right*) that could be encoded by neural responses. Each grooming signal was smoothed using a 30 s window (we obtained qualitatively similar results on varying this choice). *First row:* Variables encoding cumulative time spent in grooming: Grooming Surplus Time (GST) overlaid with Cumulative Giving Grooming Time (CGGT) and Cumulative Receiving Grooming Time (CRGT). Note that GST = CGGT – CRGT.

Second row: Variables that represent counting of bouts: Grooming Surplus Number (GSN) overlaid with Cumulative Giving Grooming Number (CGGN) and Cumulative Receiving Grooming Number (CRGN).

Third row: Variables that represent binary state changes: Is Giving Grooming (IGG) and Is Receiving Grooming (IRG).

Fourth row: Variables that represent elapsed duration only within each bout: Within Bout Giving Grooming Time (WBGGT) and Within Bout Receiving Grooming Time (WBRGT)

Fifth row: Variables that represent elapsed duration of interaction regardless of give or receiving grooming: Within Bout Grooming Time (WBGT).

(B) Average correlation (mean ± s.e.m across neurons) between each grooming variable with average firing rate of IT neurons (n = 243 from M1 & M2). White asterisks indicate statistically significant correlations (* is $p < 0.05$, ** is $p < 0.005$, etc., sign-rank test across neurons). Asterisks above each pair of bars indicate statistically significant comparisons (* is $p < 0.05$, ** is $p < 0.005$, etc., sign-rank test across neurons).

(C) Same as (B) but for PMv (n = 185 across M1 & M2)

(D) Same as (B) but for PFC of M1 (n = 61 in M1)

(E) Average partial correlation (mean ± s.e.m across neurons) between each grooming variable and average firing rate after controlling for all other factors for IT neurons (n = 243 from M1 & M2). Asterisks follow the same convention as before.

(F) Same as (E) but for PMv (n = 185 across M1 & M2)

(G) Same as (E) but for PFC of M1 (n = 61 in M1)

SECTION S3. SPIKE & LFP POWER SPECTRA ACROSS GROOMING TYPE

Introduction

We found that IT & PMv show elevated firing while each monkey is grooming his partner compared to when it receives grooming. Here, we investigated whether these firing rate increases are driven by increased power in specific frequency bands, by calculating the power spectrum as a function of frequency. In addition, we also investigated whether the increased firing rates during grooming are accompanied by changes in the frequency of local field potential oscillations in each brain region.

Methods

Local field potentials (LFP) were extracted from the wideband signal recorded from each electrode by band-pass filtering the signal in the window [0.3 500] Hz and down-sampling to 2500 samples/s., whereas the multiunit activity (MUA) was extracted from the wideband signal by using Plexon Offline Sorter. We observed high amplitude fluctuations in some of the electrodes in MUA & LFP data, and therefore removed them from further analysis. In all, we analyzed LFP signals from 215 electrodes in IT, 153 in PMv and 60 in PFC, and analyzed MUA from 243 neurons in IT, 185 in PMv and 61 in PFC across two monkeys.

We computed the power in the MUA and LFP signal from each electrode using the MATLAB function *'pspectrum'* (using 1-second time resolution, no overlap), and averaged the power across all time bins of each grooming type (giving & receiving grooming) to obtain a global average power at each frequency for each electrode. MUA firing rates were obtained by calculating the spike counts in bins of 1/2500 s, so as to match the sampling rate of the LFP signal and make the spectra more comparable.

Results

The average MUA & LFP power spectra across all neurons for each brain region and each grooming type is shown in Figure S3. Below we describe the effects observed in each brain region.

Average MUA & LFP power spectra in IT

In monkey M1 MUA, we observed a decrease in power around the alpha band (8-12 Hz) in giving compared to receiving grooming, and an increase in power at high frequencies greater than 24 Hz (Figure S3A). In monkey M1 LFP, we observed the opposite pattern (Figure S3B): there was decreased power in all frequencies during giving grooming, with the effect particularly pronounced in the alpha band and in around 39 Hz. Thus, there is increased alpha power during receiving grooming in both firing rate and local field potentials, which might be due to monkey M1 closing his eyes or relaxing while receiving grooming from his partner.

In monkey M2, we observed a wideband increase in MUA power in the giving compared to receiving grooming condition. This was accompanied by a selective decrease in alpha power in LFP and an increase in power around 63 Hz (Figure S3B). Thus, there is increased alpha power during receiving grooming in M2 but only in LFP but not in the firing rate.

Thus, the increased firing rate in IT during giving grooming is accompanied by

decreased LFP power particularly in the alpha band. We speculate that this could be due to increased inhibitory synaptic input during receiving grooming, driven by alpha band oscillations.

Average MUA & LFP power spectra in PMv

In monkey M1 MUA, we observed consistently larger power in giving grooming at all frequencies (Figure S3C), with the smallest effect in the alpha band. By contrast, the LFP power was consistently smaller in giving grooming compared to receiving grooming, with the largest effect around 20 Hz (Figure S3D).

In monkey M2 MUA, there was uniformly larger power in giving grooming at all frequencies (Figure S3C). By contrast, the LFP power was smaller in giving grooming around 24 Hz and larger in higher frequencies around 42 Hz (Figure S3D).

Thus, the increased firing rate in PMv during giving grooming is accompanied by reduced LFP power particularly in the alpha band. We speculate that this could be due to increased inhibitory synaptic input during receiving grooming, driven by alpha band oscillations.

Average MUA & LFP power spectra in PFC

In monkey M1 MUA, we observed lower power during giving grooming at all frequencies (Figure S3E). This was accompanied by reduced LFP power during giving grooming compared to receiving grooming, with the effect most prominent in the alpha band (Figure S3F). We speculate that this could be due to increased PFC activity during receiving grooming when the monkey is directing the grooming of his partner towards desirable locations.

Dynamics of MUA & LFP spectra across brain regions

To characterize the dynamics of these spectral power variations across time, we visualized the power spectrum for each bin separately for MUA (Figure S4) and for LFP signals (Figure S5). It can be seen that there are specific times at which the spectral power is modulated even within grooming bouts, and that there is greater spectral power during giving grooming in MUA (Figure S4) and greater spectral power during receiving grooming in LFP (Figure S5).

Conclusions

We conclude that both IT & PMv show increased firing rates during giving grooming, which is accompanied by decreased LFP power, particularly in the alpha band. We speculate that this could be due to increased inhibitory synaptic input during receiving grooming, driven by alpha oscillations.

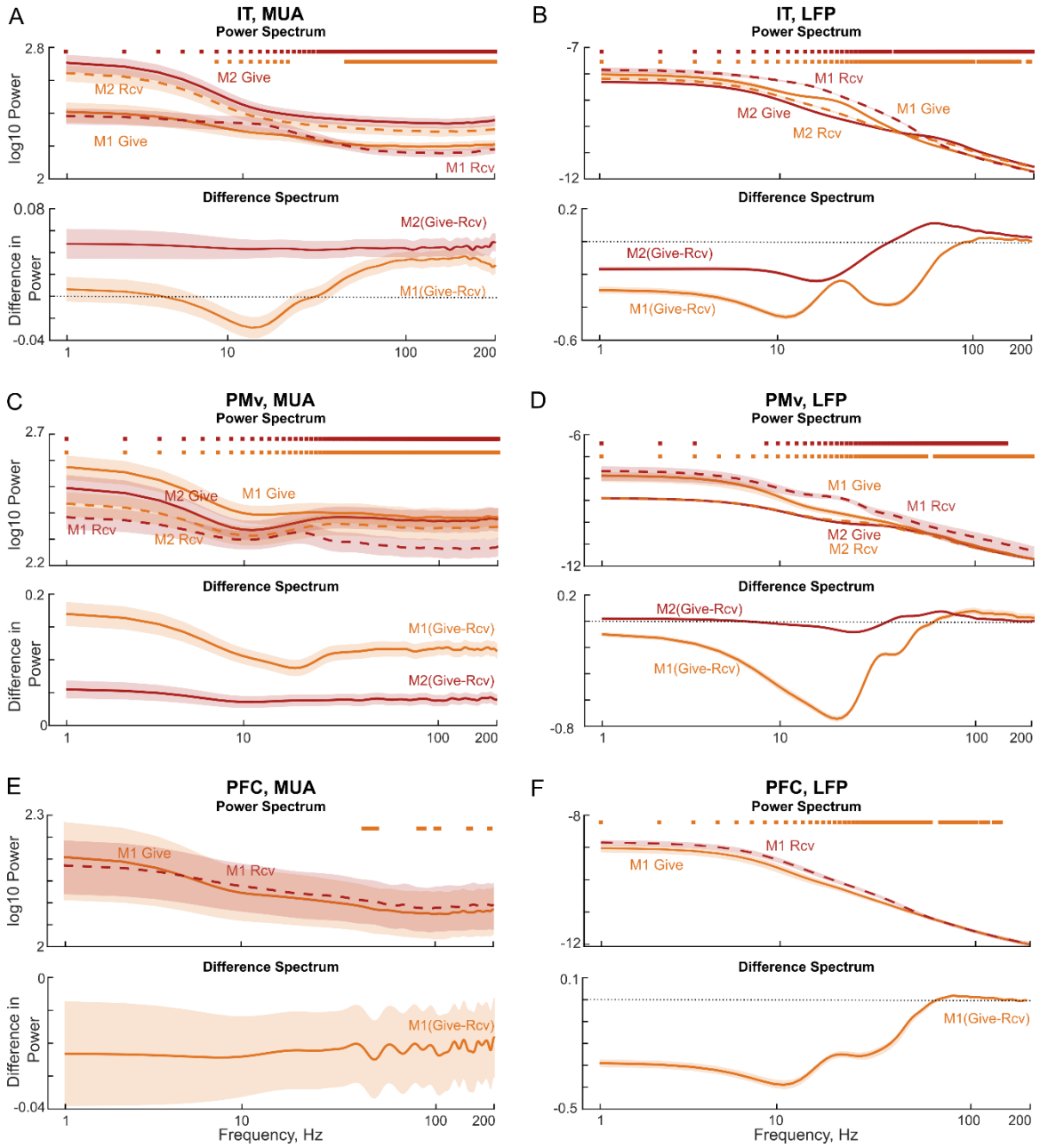

Figure S3. Multiunit activity & local field power spectra across grooming types

(A) *Top:* Average power spectrum of multiunit activity (MUA) across all IT neurons in give & receiving grooming conditions in M1 (n = 118) and M2 (n = 125). Shaded regions indicate s.e.m across neurons. The squares at the top indicate statistically significant differences in power at each frequency (sign-rank test, $p < 0.05$). *Bottom:* Difference in the power between give and receiving grooming for M1 & M2

(B) Same as A, but for local field potentials (LFP) in IT cortex from M1 (n = 106) and M2 (n = 109)

(C) Same as A, but for MUA in PMv in M1 (n = 57) and M2 (n = 128).

(D) Same as B, but for LFP in PMv cortex of M1 (n = 43) and M2 (n = 110)

(E) Same as A, but for MUA in PFC of M1 (n = 61).

(F) Same as B, but for LFP in PFC of M1 (n = 60).

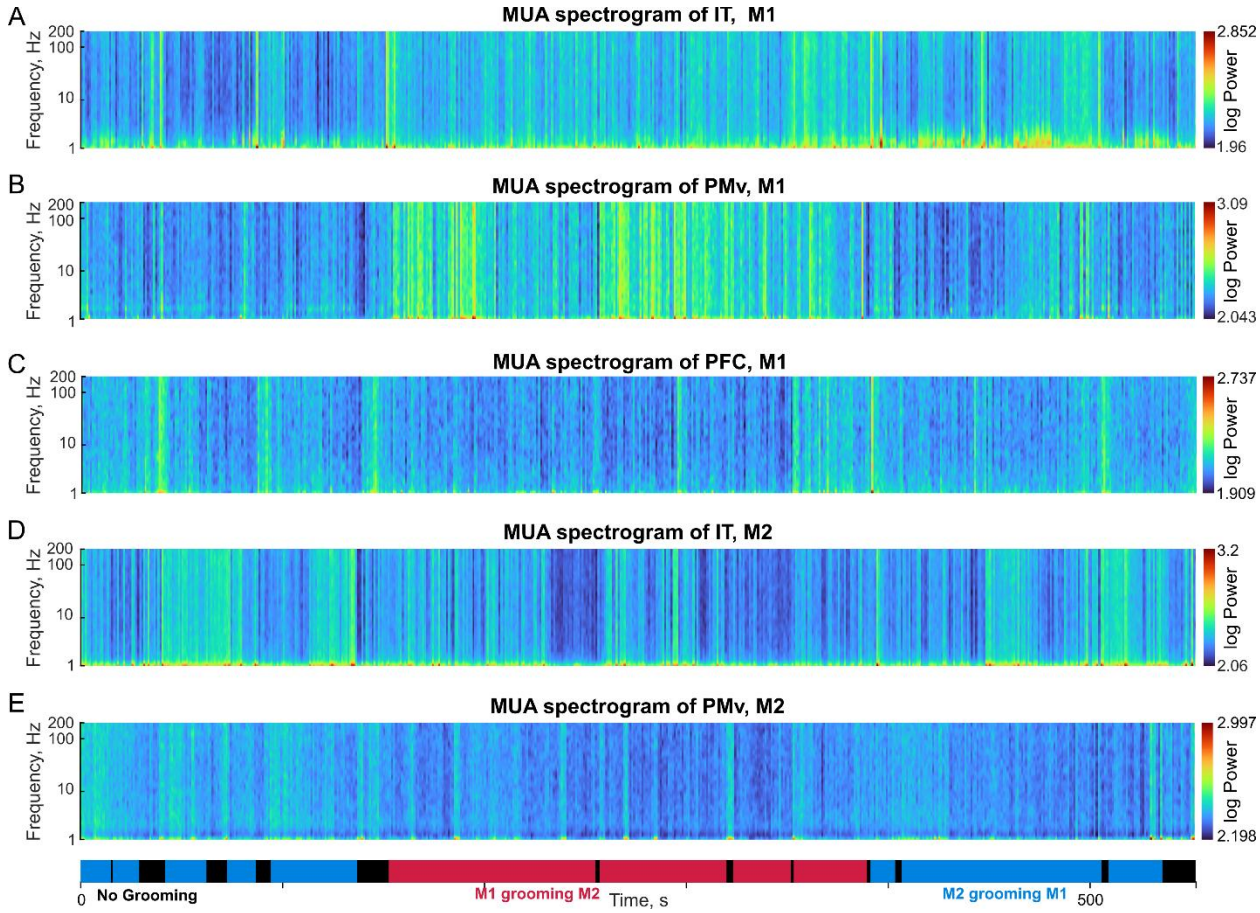

Figure S4. MUA spectrogram during the social interaction

(A) Spectrogram of the multiunit (MUA) activity in IT cortex of monkey M1 averaged across neurons (n = 118). Frequency is shown along the y-axis on a logarithmic scale. The plot on the bottom shows the timeline of the social interaction with the three types of grooming behaviors: M1 grooming M2 (*red*), M2 grooming M1 (*blue*) and no grooming (*black*).

(B) Same as (A) but for PMv of M1 (n = 57)

(C) Same as (A) but for PFC of M1 (n = 61)

(D) Same as (A) but for IT of M2 (n = 125)

(E) Same as (A) but for PMv of M1 (n = 128)

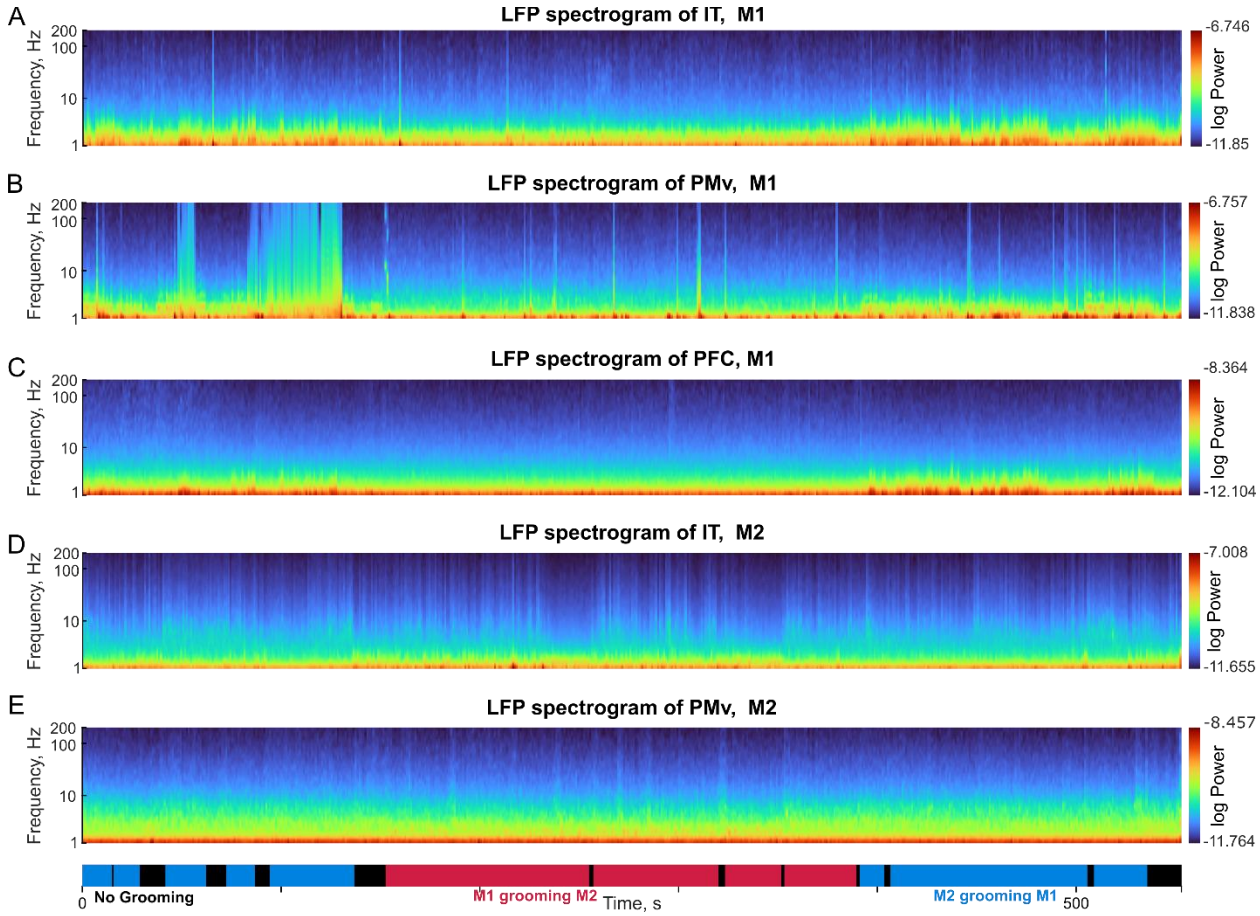

Figure S5. LFP spectrogram during the social interaction

(A) Spectrogram of local field potential (LFP) activity in IT cortex of monkey M1 averaged across neurons (n = 106). Frequency is shown along the y-axis on a logarithmic scale. The plot on the bottom shows the timeline of the social interaction with the three types of grooming behaviors: M1 grooming M2 (*red*), M2 grooming M1 (*blue*) and no grooming (*black*).

(B) Same as (A) but for PMv of M1 (n = 43)

(C) Same as (A) but for PFC of M1 (n = 60)

(D) Same as (A) but for IT cortex of M2 (n = 109)

(E) Same as (A) but for PMv of M2 (n = 110)

SECTION S4. GROOMING DECODING ACROSS TRANSITIONS

We found that neural activity can be used to decode the ongoing grooming state during the social interaction (Figure 3). While this is expected since each state involves distinct sensory inputs and motor outputs, a more interesting possibility is that neural activity also carries information about an upcoming transition from one grooming state to another.

To investigate this issue, we calculated the grooming decoder probabilities in successive 0.5 s bins in a 31 s window around each transition: from No Grooming to Giving grooming and vice versa (Figure S6A) and from No Grooming to Receive Grooming and vice-versa (Figure S6B). In all cases, we found a gradual transition whereby the decoder probability increased a few seconds before the transition itself. These changes could well be due to changes in behavior of the animals as they prepare for the transition, or due to preparatory neural activity that is commonly found to precede motor movements.

Thus, neural activity carries information about the future grooming state around the time of a transition.

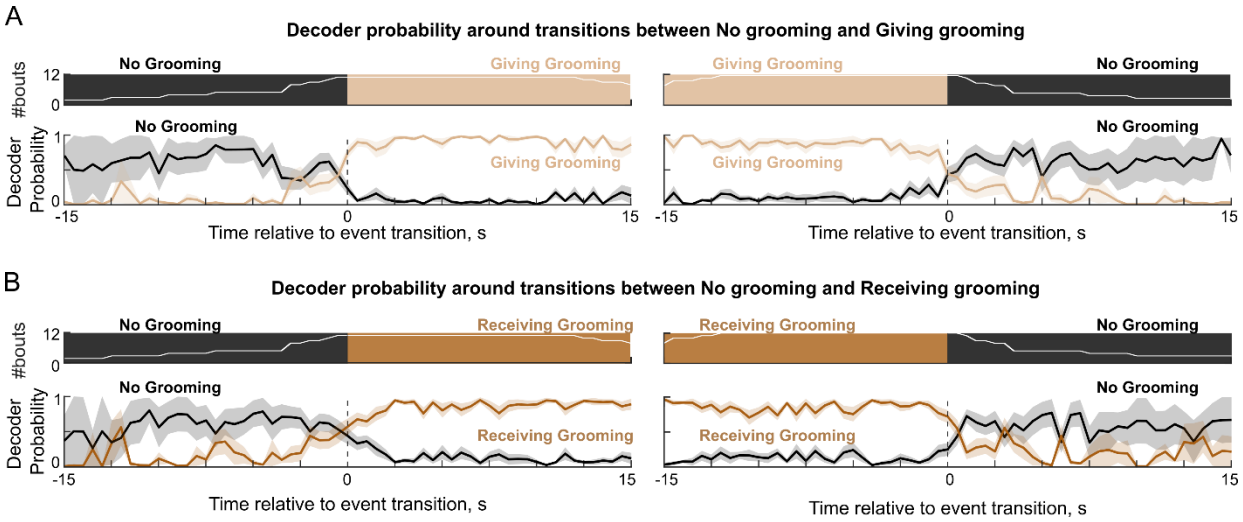

Figure S6. Grooming state decoding during transitions between grooming bouts. Average grooming state decoding probability around the time of transitions from one grooming type to another. The *top row* in each panel shows the number of bouts included at each point in time relative to the event transition, and the bottom row depicts the grooming decoder probability averaged across these number of bouts. Shaded bars represent s.e.m across bouts.

(A) *Left:* Grooming state decoding probability for giving grooming (in brown color) and no grooming (in black color) around the transition from no grooming to giving grooming. *Right:* Same as earlier, but for the transition from giving grooming to no grooming.

(B) Same as (A) but in place of giving grooming, receiving grooming probability is plotted for transitions from no grooming to receiving grooming (*left*) and from receiving grooming to no grooming (*right*)

SECTION S5. DYNAMICS OF PARTNER AND HAND DECODING

Dynamics of partner identity decoding during social interaction

We have found that partner identity could be reliably decoded from IT neurons with no systematic differences across different type of grooming bouts (Figure 4). To investigate whether this decoding was stable throughout time, we calculated the face decoding accuracy as a function of time from both monkey M1 IT (Figure S7A) and monkey M2 IT (Figure S7B). We found that face decoding accuracy changed dynamically throughout the session, presumably higher when the monkeys looked at each other or were tracking each other. Thus, IT neurons show stable decoding of partner identity throughout the social interaction with interesting variations in overall accuracy depending on what the animal is looking into.

Dynamics of hand decoding during the social interaction

Since each monkey performed a motor task with his left and right hand (see Methods), we wondered whether it would be possible to decode the hand that is being used during the social interaction. To this end, we trained a 2-way decoder on the motor task responses in each brain region using the same methods as before, and tested it during times during the social interaction when we annotated each monkey using his left or right hand (Figure S8A). We found that hand decoding was accurate only in PMv (Figure S8B).

To investigate the dynamics of hand decoding, we calculated the hand decoding probability across time using the PMv activity in each monkey. Since, in our manual annotation, we specified the left/right hand usage only when the monkey initiated the grooming, the hand labels are not available for the entire recording. Hence, we show the probability of left hand label, instead of accuracy (Figure S8 C,D). We smoothened the probability of left hand label, in a window of 5 s with a step size of 1 s. The mean and s.e.m. of the probability values in each 5 s window is shown (Figure S8 C,D top plots) This revealed dynamic variations in hand decoding probability which corresponded nicely to the left or right hand being used by each monkey for grooming during the social interaction (Figure S8 C-D).

Thus, there is a systematic relationship between neural activity evoked during more controlled motor tasks and the motor movements that occur during social interaction.

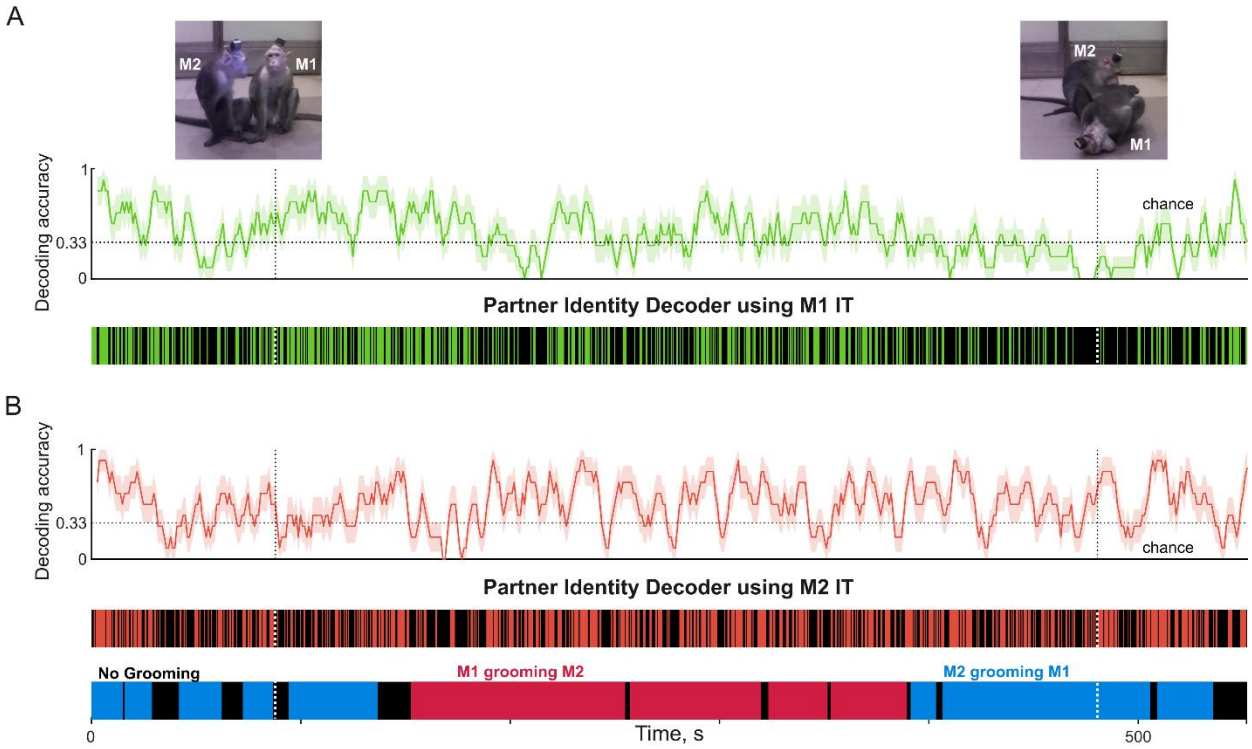

Figure S7. Dynamics of partner identity decoding during social interaction

(A) *Top:* Decoding accuracy of partner identity decoding, calculated across 5 s bins with a step size of 1 s from M1 IT neurons, with example frames illustrating the two monkeys when they are facing each other, and when they are not facing each other. *Bottom:* Decoding accuracy in individual time bins throughout the social interaction session (*green*: correct, *black*: incorrect)

(B) Same as (A) but using monkey M2 IT neurons (*red*: correct, *black*: incorrect).

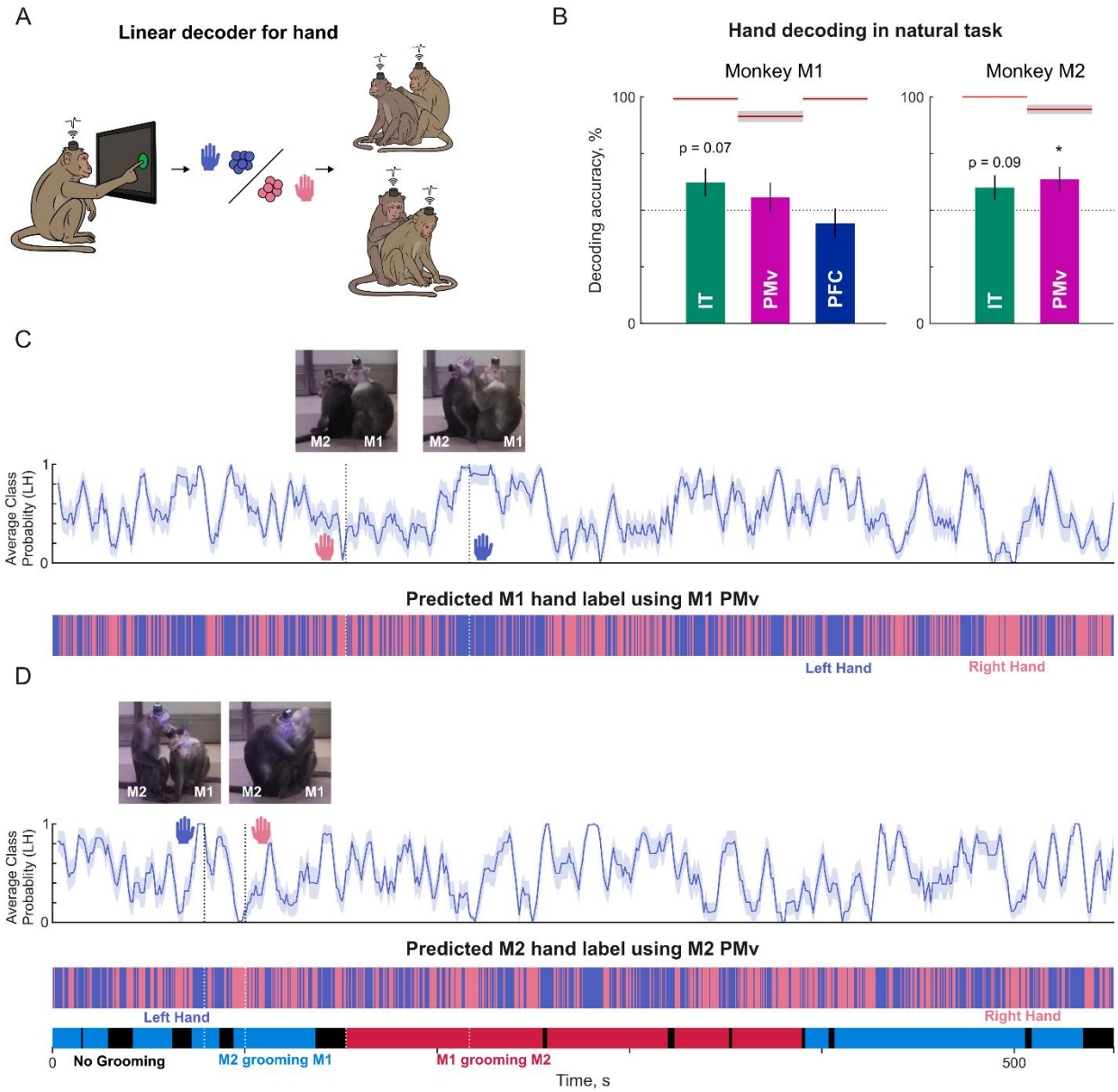

Figure S8. Dynamics of hand decoding during social interaction

(A) *Left:* Schematic of the motor task performed by each monkey separately, where he had to touch a target appearing on the screen with his left hand or right hand. *Middle:* We trained a two-way linear decoder on the neural responses on the motor task to decode which hand is being used by the monkey. *Right:* We tested the decoder during the social interaction.

(B) Hand decoding accuracy from monkey M1 (IT, PMv & PFC) and from monkey M2 (IT, PMv). Red lines indicate decoding accuracy from the motor task, with shaded regions representing s.e.m across trials. Asterisks represent statistical significance of the decoding accuracy being above chance level ($p < 0.05$, chi-square test across 21 bins & 1 instances of left hand & 40 bins and 2 instances of right hand in M1 and 40 bins & 2 instances of left hand & 40 bins and 2 instances of right hand)

(C) *Top:* Average class probability given by the decoder for 'Left Hand' label,

calculated across 5 s bins with a step size of 1 s from M1 PMv neurons, with example frames illustrating various types of hand use. *Bottom:* Predicted hand label in individual time bins throughout the social interaction (*pink*: right hand, *blue*: left hand)

(D) Same as (A) but using monkey M2 PMv neurons.

SECTION S6. ADDITIONAL ANALYSIS OF SELF & PARTNER JOINT MODELS

Self and partner joint model correlations for different levels of joint motion

We have found that neural activity in each monkey is predicted better by the partner's joint positions during giving grooming and by his own joints during receiving grooming (Figure 5). However, these self and partner joint correlations could be modulated by the amount of motion in these joints, which could be different between give and receiving grooming.

To investigate this issue further, for each joint, we calculated the motion energy by taking the absolute difference between the joint position of each bin with the next bin. We then calculated the z-scored motion signal from each joint position, and averaged it across joints to obtain an average motion signal. We then calculated the difference in cross-validated model correlation between self and partner joint models for different levels of self and partner motion (in quartiles). The resulting plots are shown in Figure S9.

We found qualitatively similar results for all levels of joint motion (Figure S9). In other words, during giving grooming, neural activity of the groomer was predicted better by the partner's joints and vice-versa during receiving grooming. However, when the monkeys' own joints had higher motion strength, we found that the self joint model predicted neural activity better (Figure S9).

Dynamics of self & partner joint correlations with time

To investigate the dynamics of the self and partner joint models across time for all neurons, we calculated instantaneous correlations between the observed and predicted firing rates of all neurons (after excluding the noisy ones). We averaged the instantaneous correlation values in 5 s time windows in time steps of 1 s. The time course of the difference between self and partner joint model correlations is shown for each region in Figure S10. We find distinct periods within each grooming bout in which the partner model has a higher correlation compared to the self-joint model, complementing our observation that the partner drives grooming in social interactions.

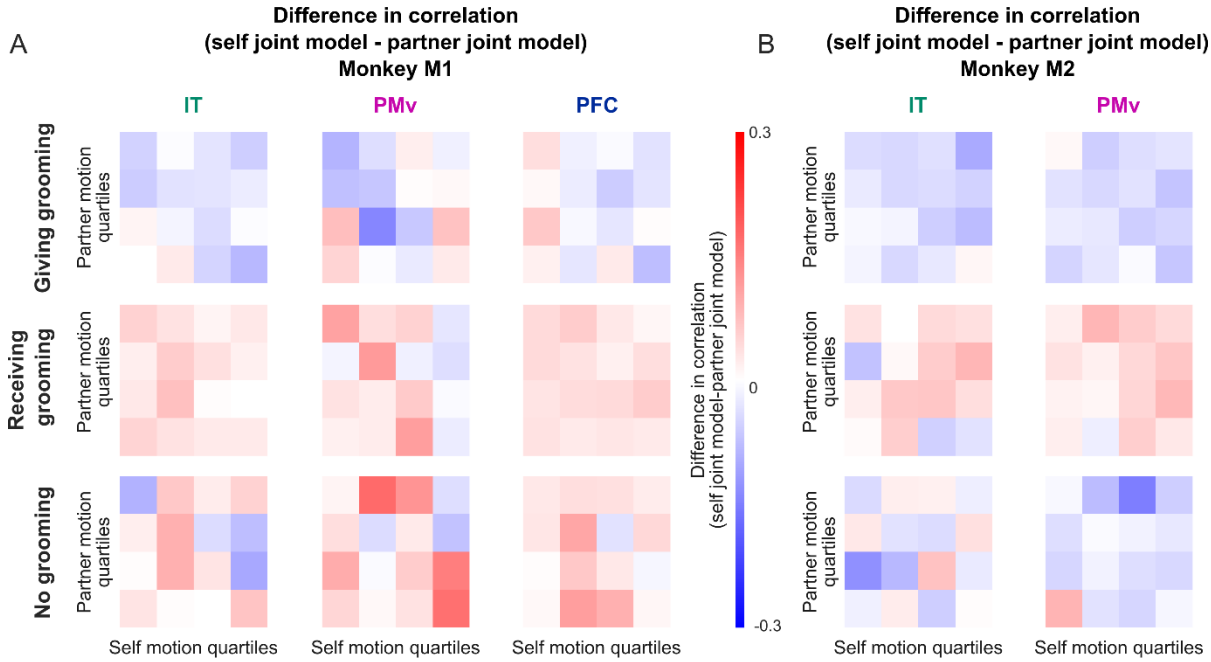

Figure S9. Self & partner model correlations for different levels of joint motion

(A) Difference between self and partner joint model correlations in IT (*left*), PMv (*middle*) and PFC (*right*) monkey M1 for giving grooming (*top*), receiving grooming (*middle*) and no grooming (*bottom*) bins of the social interaction. Each color map contains the difference in the model correlations for each quartile of self and partner motion, with *red* indicating self joint model correlation being larger than the partner model, and *blue* indicating the opposite.

(B) Same as (A) but for monkey M2.

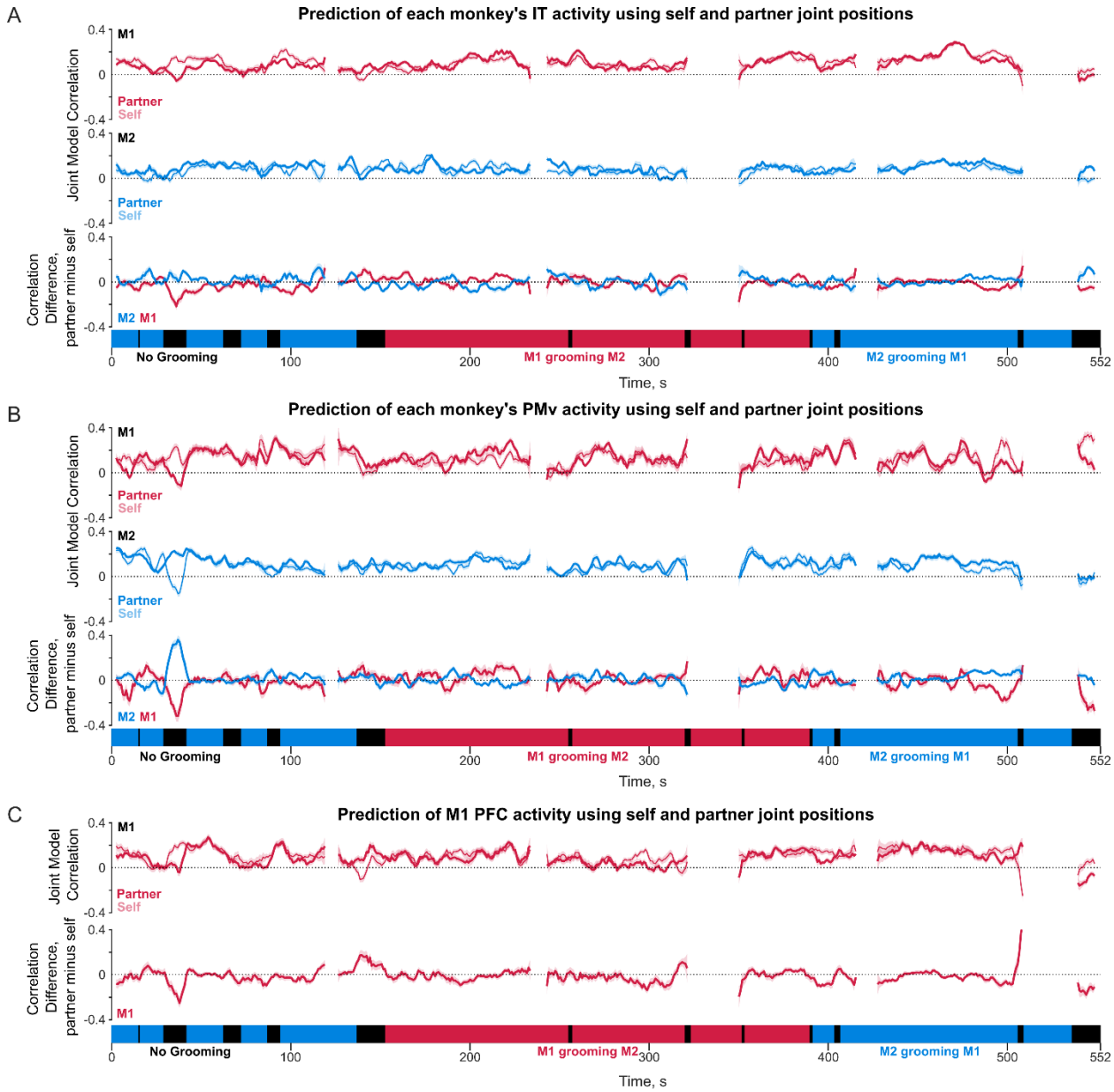

Figure S10. Time course of self & partner joint correlations during social interaction.

(A) Top. Time course of smoothened instantaneous correlation of the partner *(darker)* and self *(lighter)* joint models in IT for M1, with shaded bars representing s.e.m across average correlation within moving window of 5s. Middle. Same as Top, but for M2. Bottom. Difference between partner and self joint model correlation plotted over time for M1 (red) and M2 (blue) separately.

(B) Same as (A) but for PMv

(C) Same as (A) but for PFC.

SECTION S7. INTERBRAIN COUPLING DYNAMICS ACROSS BRAIN REGIONS

We have found that brain activity of the groomer is driven the receivers brain activity for PMv & PFC considered together. Here we report the interbrain coupling for each brain region separately (Figure S11).

In IT, we found that the brain activity of the groomer is predicted by the receiver only slightly better than the other way around, and this effect did not attain statistical significance (Figure S11A). Upon computing these partner model correlations as a function of time, we found distinct periods where the neural activity of each monkey is strongly predicted by his partner (Figure S11B). We speculate that these could be periods where both monkeys are looking at common visual items in their environment, or at each others movements.

In PMv, we found that the brain activity of the groomer is predicted by the receiver, and this effect was statistically significant (Figure S11C). Here too, we found the neural activity of each monkey to be strongly predicted at some phases during the social interaction compared to others (Figure S11D). We speculate that these could be periods when the monkey was closely tracking the movements of his partner.

Finally, in PFC, we have brain recordings only from M1, but here we find that PFC neurons were predicted better by M2 neural activity during M2 grooming M1 compared to when M1 groomed M2, but this did not reach significance ($p = 0.93$) Here too, we found neural activity of M1 to be strongly driven by his partner at some times during the social interaction compared to others (Figure S11F). We speculate that these could be periods of shared visual attention or goals, or shared tracking of each other's movements.

Taken together, we find that interbrain coupling exhibits rich dynamics across the course of the social interaction, and these dynamics are largely driven by the receiver of the grooming.

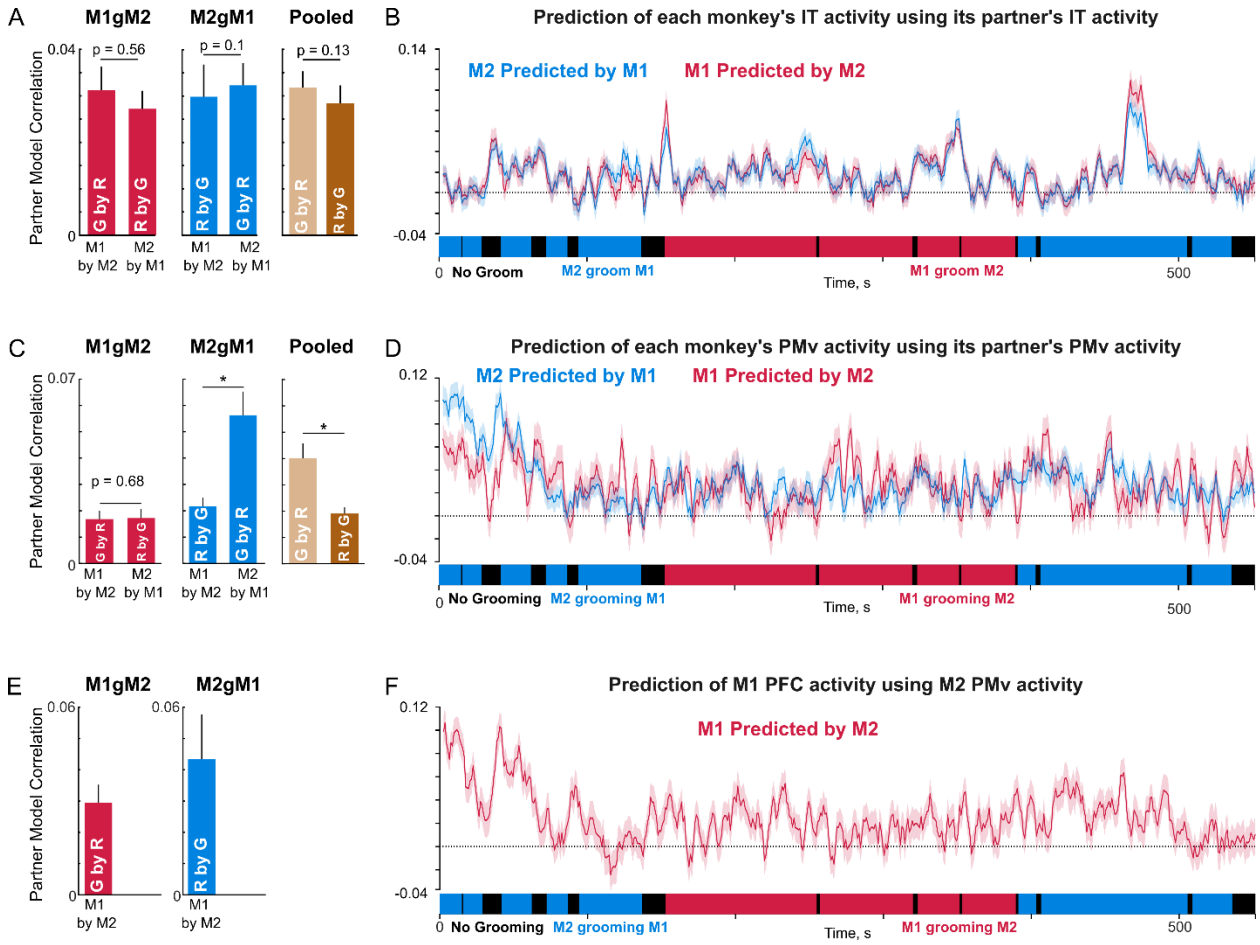

Figure S11. Dynamics of interbrain coupling across brain regions

(A) Partner model correlation (mean + s.e.m) in IT cortex of M1 & M2 while M1 groomed M2 (*left, red bars*), while M2 groomed M1 (*middle, blue bars*), and pooled data for the groomer and receiver monkey (*right, brown bars*), across the neurons which show significant model correlation. Asterisks indicate statistically significant comparisons (* is $p < 0.05$, Wilcoxon rank sum test across neurons). 'G by R' indicates the average correlation across neurons when groomer's brain activity is predicted by receiver's brain activity and 'R by G' indicates the average correlation across neurons when the receiver's brain activity is predicted by the groomer's activity.

(B) Time course of partner model correlation during the entire interaction (mean ± s.e.m, solid lines with shaded regions across all 50 ms time bins in the 5 s smoothening window).

(C-D) Same as (A) & (B) but for PMv cortex of M1 & M2.

(E-F) Same as (A) & (B) but for PFC of M1.

SECTION S8. INTERBRAIN CROSS-CORRELATION

We have found that the groomer's brain activity is predicted by the receiver's brain activity in both monkeys (Figure 6). However, this analysis is based on instantaneous activity and does not account for possible temporal relationships (like a lead or lag) between the two brains, or possible coherence in specific frequency bands. Here, we investigate these possibilities. We did not find clear patterns, but nonetheless included detailed analyses here for the sake of completeness.

Inter-brain cross-correlation dynamics during social interaction

We began by asking whether there is any temporal relationship between the neural activity in the two monkeys during the social interaction. For instance, the neural activity of the groomer could precede the neural activity of the receiver since the groomer initiates motor movements whose sensory consequences are registered in the receiver's brain.

To this end, we computed the cross-correlation between every possible pair of neurons in the IT cortex of the two monkeys (118 IT neurons in M1 x 125 IT neurons in M2 = 14750 pairs in MUA). For each pair, we computed the firing rate of the two neurons in 10 ms bins, and calculated their cross-correlation within a time window of 2 s with a maximum lag of 1 s. The average cross-correlogram between all IT neuron pairs (n = 14,750) is shown in Figure S12A. It can be seen that the cross-correlation shows rich dynamics with time, although we did not observe any link to key behavioral events or grooming states.

To further characterize these cross-correlation dynamics, we first grouped the time bins into the three types of grooming behaviors (M1 grooming M2, M2 grooming M1 and no grooming), and calculated the cross-correlogram for each grooming type. The resulting cross-correlogram showed no clear differences across grooming type (Figure S12B). Next, we identified the lag at which there was a peak in the average cross-correlation. The resulting peak average cross-correlation (Figure S12C) varied with time, showing the largest cross-correlation for M2 grooming M1, followed by No Grooming, and then by M1 grooming M2 (Figure S12D). Finally, we also calculated the peak lag across time (Figure S12E) which did not show any systematic variation with grooming types (Figure S12F). Interestingly, both give and receiving grooming conditions had a positive lag, meaning that M2 activity precedes M1 activity in both conditions, for reasons that are not clear to us.

We repeated these analysis for PMv-PFC pairs (118 PMv/PFC neurons in M1 x 128 PMv neurons of M2 = 15104 pairs). We grouped PMv & PFC together so that there would be roughly equal numbers of neurons in M1 & M2, after finding the results to be qualitatively similar even without grouping. We observed less temporal variations in the average cross-correlogram compared to IT (Figure S12G), with no systematic differences between grooming bouts (Figure S12H) and in peak average correlations (Figure S12I-J). However with peak lags, we observed a negative mean lag in the M2 grooming M1 condition, indicating that M2 activity was lagging behind M1 (Figure S12L), consistent with our main finding that the receiver of grooming drives the social interaction.

Finally, we repeated these analyses using the LFP signal isolated from each electrode (106 M1 IT neurons x 109 M2 IT neurons = 11554 neuron pairs; 103 M1 PMvPFC neurons x 110 M2 PMv neurons = 11330 pairs; Figure S13). We subsampled

the data (in 10 ms bins as done for MUA), for the ease of processing. Here too, we did not observe any systematic differences in cross-correlation dynamics between the different grooming types.

In sum, we conclude that there are rich dynamics of cross-correlation between both brains during social interaction, but these dynamics are not clearly interpretable at least to the best of our efforts.

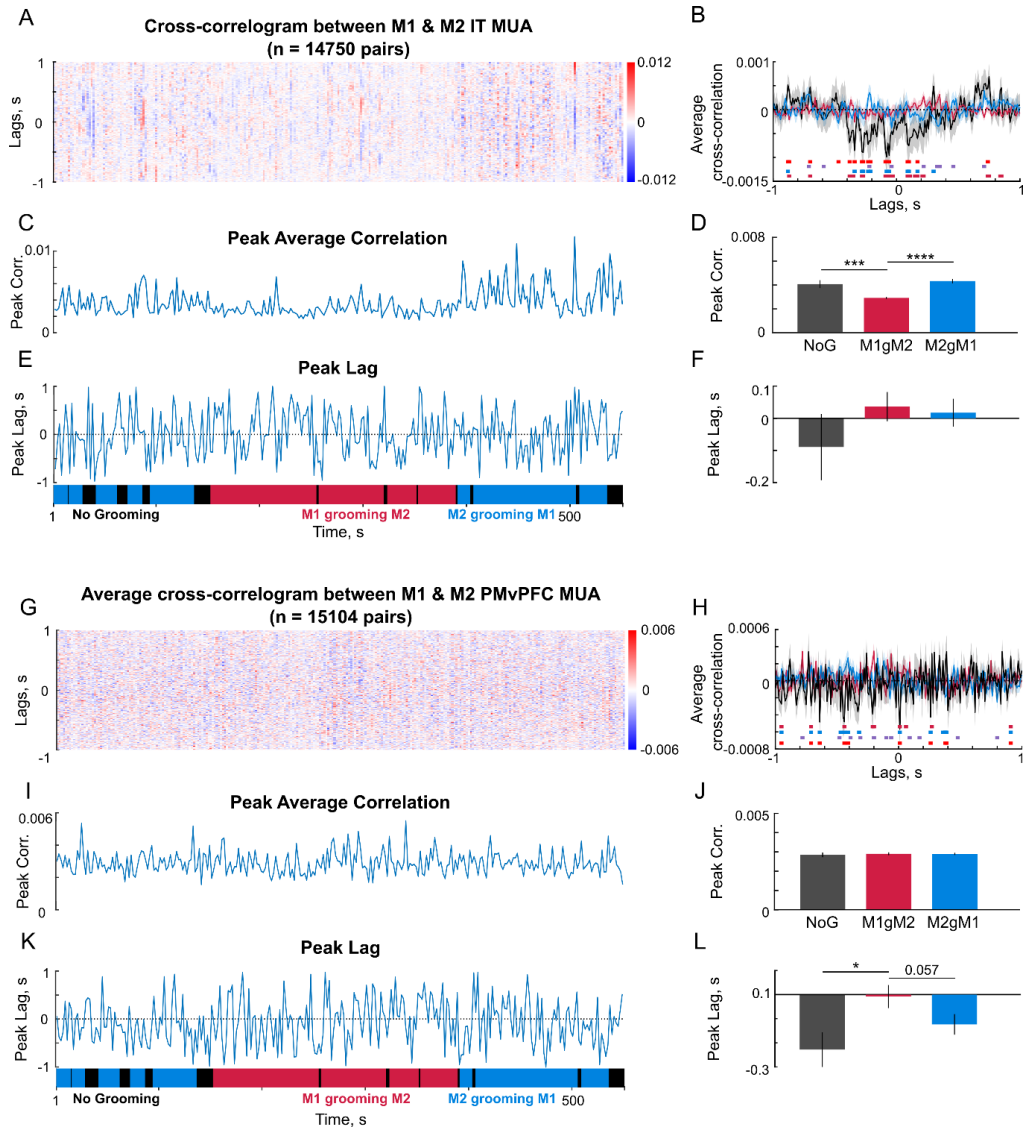

Figure S12. MUA cross-correlation dynamics during social interaction

(A) Colormap of average cross-correlogram at each lag across IT neuron pairs across time. Positive lags indicate M2 activity precedes M1 activity and negative lags indicate the opposite.

(B) Average cross-correlogram in the three different grooming conditions. The horizontal lines indicate the lags at which the median cross-correlation differs significantly between various grooming conditions ($p<0.05$, rank sum test): Blue – M1gM2 vs No grooming, Pink – M2gM1 vs No grooming, Purple – M1gM2 vs M2gM1, Red – [M1gM2, M2gM1 combined] vs No grooming.

(C) Peak of the average cross-correlation across time.

(D) Average of the peak cross-correlation for each grooming type. Error bar indicate s.e.m. of the peak correlation across time bins.

(E) Peak lag (time at which average cross-correlation attains a peak) across time.

(F) Average peak lag for each grooming type. Error bars indicate s.e.m across time bins.

(G-L) Same as (A-F) but for PMv/PFC neuron pairs.

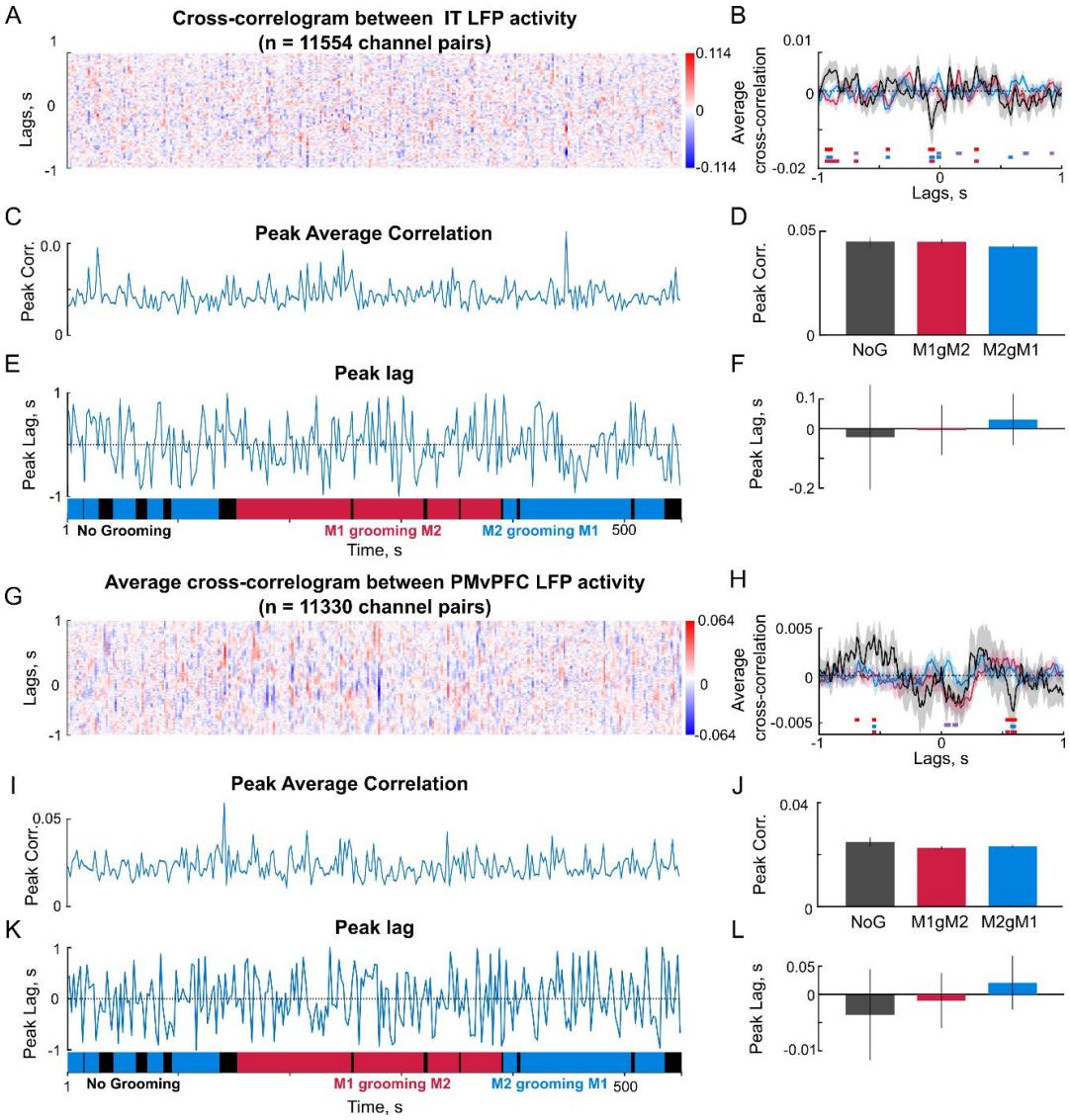

Figure S13. LFP cross-correlation dynamics during social interaction.

(A) Colormap of average cross-correlation at each lag across IT electrode pairs across time. Positive lags indicate M2 activity precedes M1 activity and negative lags indicate the opposite.

(B) Average cross-correlogram in the three different grooming conditions. The horizontal lines indicate the lags at which the median cross-correlation differs significantly between various grooming conditions ($p<0.05$, rank sum test): Blue – M1gM2 vs No grooming, Pink – M2gM1 vs No grooming, Purple – M1gM2 vs M2gM1, Red – [M1gM2, M2gM1 combined] vs No grooming.

(C) Peak of the average cross-correlation across time.

(D) Average of the peak cross-correlation for each grooming type. Error bar indicate s.e.m. of the peak correlation across time bins.

(E) Peak lag (time at which average cross-correlation attains a peak) across time.

(F) Average peak lag for each grooming type. Error bars indicate s.e.m across time bins.

(G-L) Same as (A-F) but for PMv/PFC neuron pairs

604 **Inter-brain coherence dynamics during social interaction**
605 We next investigated whether there is interbrain coupling in specific frequency
606 bands during the social interactions. Specifically we asked if there is a consistent phase
607 relationship between the frequency content of neural firing rate or local field potentials,
608 and whether there are any differences between the different grooming types.
609
610 *Methods*
611 We calculated the coherence between the MUA signal on every pair of electrodes
612 in a given brain region, and averaged it across electrodes to get a global measure. We
613 used MATLAB function "mscohere" to compute coherence, with the following set of
614 parameters: Hamming Window of size 2048 samples, which comes to 0.82 s of data with
615 a sampling rate of 2500 samples/s, and an overlap of 512 samples (0.25% overlap). This
616 set of parameters gave a frequency resolution of 1.22 Hz. For the LFP signal, we used
617 the same method as above to compute the coherence between every pair of neurons in
618 a given brain region.
619
620 *Results*
621 We first visualized the coherence in the MUA signal between IT neuron pairs
622 between the two monkeys across time in each brain region (Figure S14A). To assess
623 whether the coherence is different for different grooming types, we averaged this
624 coherence across time bins of each grooming type. This revealed significant differences
625 in coherence at low frequencies between the different grooming conditions (Figure S14B).
626 Since we did not observe differences in specific frequencies, we calculated the average
627 coherence signal as a function of time after averaging across frequencies (Figure S14C).
628 This revealed that there was significantly larger coherence during M1 grooming M2,
629 followed by M2 grooming M1 with least coherence overall in the no-grooming condition
630 (Figure S14D). We found similar results for PMvPFC neuron pairs as well (Figure S14E-
631 H).
632 We performed a similar analysis on the LFP signal (Figure S15). Although there
633 were differences in coherence at specific frequencies (Figure S15B,F), we did not find a
634 systematic difference in coherence overall (Figure S15D,F).
635 We conclude that there is increased coherence at all frequency in multiunit activity
636 during social interaction periods in all recorded regions. However, the variations in
637 coherence with time are not clearly interpretable at least to the best of our efforts.

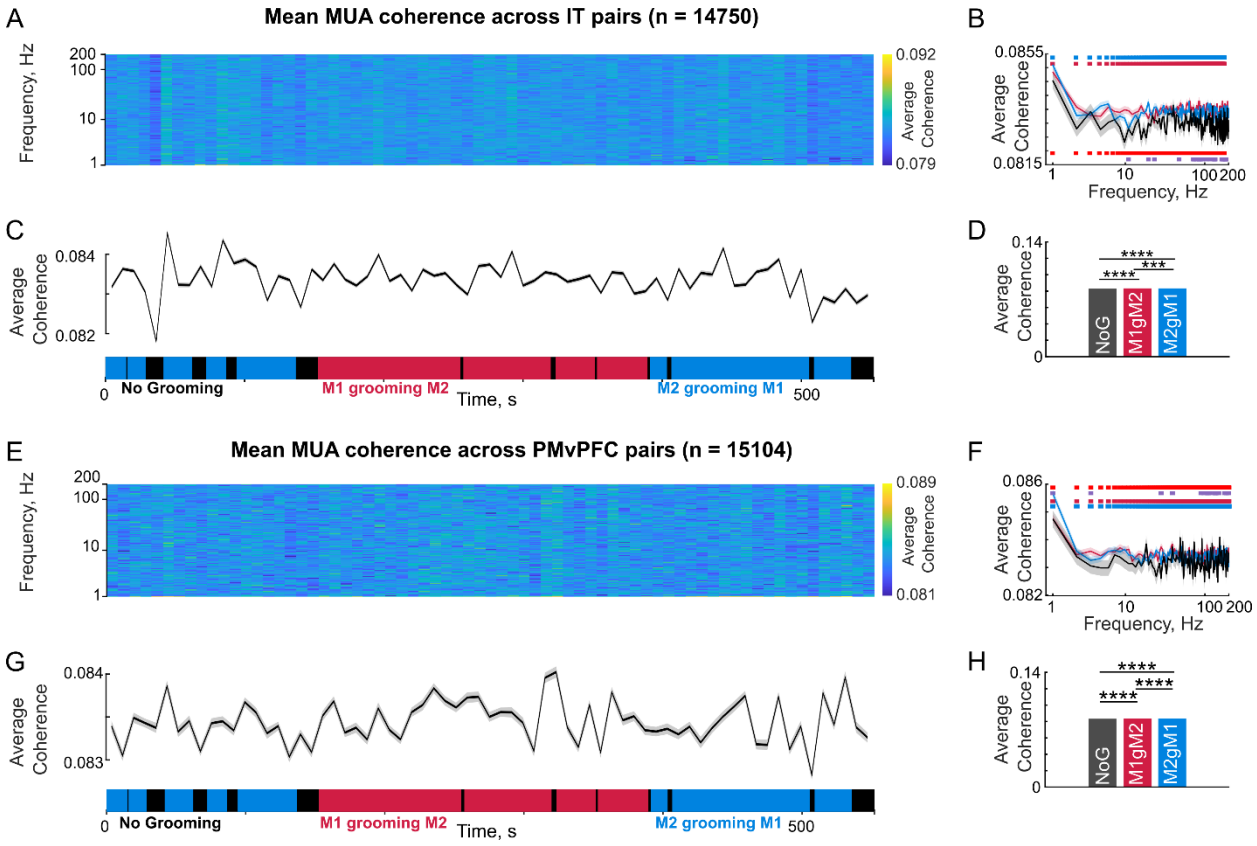

Figure S14: MUA coherence dynamics during social interaction

(A) Colormap of average magnitude-squared (ms) coherence across IT neuron pairs between the two monkeys (n = 14,750) for each frequency across time.

(B) Average coherence for each frequency across grooming conditions (M1 grooming M2, M2 grooming M1 and No grooming). The horizontal lines indicate the frequencies at which the median coherence is significantly different between various grooming conditions($p<0.05$, sign rank test): Blue – M1gM2 vs No grooming, Pink – M2gM1 vs No grooming, Purple – M1gM2 vs M2gM1, Red – [M1gM2, M2gM1 combined] vs No grooming.

(C) Average coherence in low frequencies (0-200 Hz) across time. Shaded error bars indicate s.e.m across frequency.

(D) Average coherence in low frequencies (0-200 Hz), for each grooming condition (M1 grooming M2, M2 grooming M1 and No grooming) across channel pairs. Asterisks indicate statistical significance of the comparisons (**** is $p < 0.00005$, sign rank test across neurons).

(E-H) Same as panels (A-D) but for PMvPFC pairs (n = 15,104).

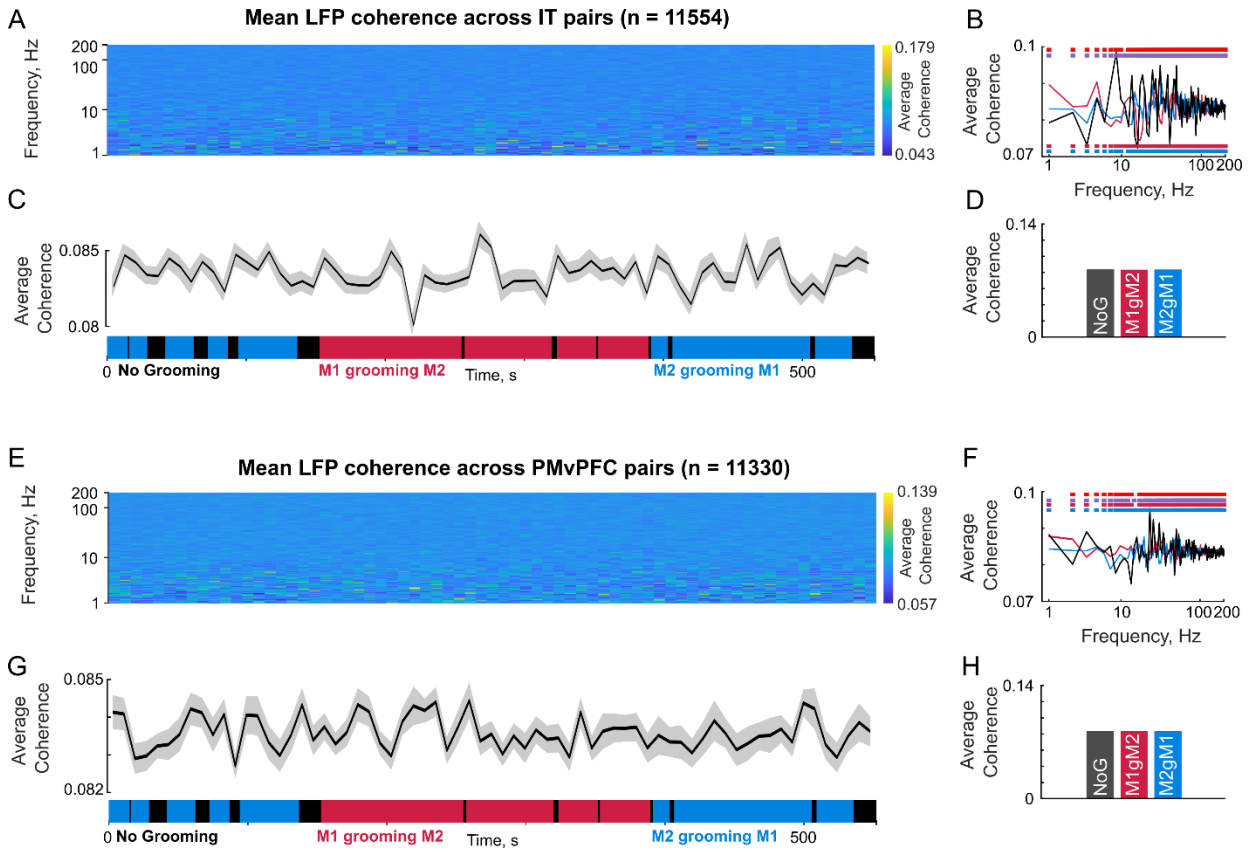

Figure S15. LFP coherence dynamics during social interaction

(A) Colormap of average LFP coherence of IT electrode pairs between the two monkeys (n = 11554) for each frequency across time.

(B) Average coherence for each frequency across grooming conditions (M1 grooming M2, M2 grooming M1 and No grooming). The horizontal lines indicate the frequencies at which the median coherence is significantly different between various grooming conditions($p<0.05$, sign rank test): Blue – M1gM2 vs No grooming, Pink – M2gM1 vs No grooming, Purple – M1gM2 vs M2gM1, Red – [M1gM2, M2gM1 combined] vs No grooming.

(C) Average coherence in low frequencies (0-200 Hz) across time. Shaded error bars indicate s.e.m across frequency.

(D) Average coherence in low frequencies (0-200 Hz), for each grooming condition (M1 grooming M2, M2 grooming M1 and No grooming) across channel pairs.

(E-H) Same as panels (A-D) but for PMvPFC pairs (n = 11330).

SECTION S9. CONVERGENCE BETWEEN BEHAVIOR AND NEURAL SIGNALS

Summary

In the main text, we have shown that neural signals like grooming surplus, partner identity, partner joints, interbrain coupling vary dynamically across the social interaction, and are modulated by the grooming state. However it is possible that key behavioral events during the social interaction have converging evidence from multiple neural signals, which might support a clear indication of each monkeys' internal state.

To this end, we carefully reviewed the behavioral events throughout the social interaction, and identified key events that we considered potentially important. At those times, we report the status of several neural signals that we considered to be relevant to the internal state of each monkey. These neural signals included

(1) Alpha power, known to be a marker for relaxation or eye closed
(2) Beta power, generally thought to be a marker for movements
(3) Partner decoding accuracy from M1 & M2 IT neurons (same as Figure S7), which could indicate the degree to which each monkey is aware of his social partner
(4) Joint model correlations for self & partner joints for M1 & M2, which could indicate the degree to which each monkey is tracking his own and his partner's joints
(5) Partner model correlation for M1 & M2, which could indicate the degree to which the two brains are coupled.

Table S1. Key behavioral events and ongoing neural signals (ref: Figure S16)

Video Time	Key Behavioral Event	Summary of Ongoing Neural Signals
145 s	M2 was grooming M1 and changed the grooming site without no obvious indication from M1.	• *Alpha power:* No clear trend. • *Beta power:* Peak in M1 IT. • *Partner decoding:* High in M1 and M2. • *Joint models:* Self & partner model high in M1, self model high in M2. • *Partner neural model:* M2 > M1 • *Interpretation:* Both M1 & M2 are tracking their partner's identity & joints.
159 to 162 s	M2 stopped grooming M1 with no obvious indication from M1 M1 was lying down and sat up as soon as M2 stopped, but did not look directly at M2.	• *Alpha power:* No clear trend. • *Beta power:* Peak in M1 PMv & M2 IT, PMv. • *Partner decoding:* High in M1, Low in M2 • *Joint models:* M1 & M2 self models are high. • *Partner neural model:* M2 > M1. • *Interpretation:* M1 is aware of M2 despite not looking directly, and M1 & M2 are not tracking their partner's joints.
168 to 172 s	M2 is not grooming M1 M1 made a sound (presumably soliciting grooming) M2 responded by resuming grooming of M1.	• *Alpha power:* Peak in M1 PMv. • *Beta power:* Peak in M1 PMv & M2 IT. • *Partner decoding:* M1 > M2. • *Joint models:* self > partner in M1, partner > self in M2, and both trends reduced over time. • *Partner neural model:* M2 > M1, but both are at a peak.

		• *Interpretation:* M1 is aware of his partner's identity, and both M1 & M2 are tracking their partner's joints.
192 to 202 s	M2 was grooming the right side of M1's face, then switched hands to hold M1's implant and bend M1's head to groom the left side of M1's face.	• *Alpha power:* No clear trend. • *Beta power:* No clear trend. • *Partner decoding:* M2 > M1. • *Joint models:* No clear trend. • *Partner neural model:* Small peak in M1 & M2. • *Interpretation:* M2 is directly seeing his partner and encoding his partner's identity, and both M1 & M2 are encoding their own joints and their partner's joints.
216 to 220 s	M2 was grooming M1's back and stopped grooming M1 momentarily. M1 turned, looked up, stretched his neck and made a small movement (presumably soliciting grooming) M2 responded by resuming grooming of M1 starting with the neck.	• *Alpha power:* Peak in M1 IT, PMv, PFC. • *Beta power:* Peak in M1 IT, PMv, PFC & M2 IT. • *Partner decoding:* M1 > M2 • *Joint models:* self & partner high in M1, partner > self in M2. • *Partner neural model:* M1 > M2 • *Interpretation:* M1 is aware of his partner's identity and his own & partner's joints. M2 is tracking his partner's joints.
266 to 282 s	M2 stopped grooming M1, and M1 turned around and began scratching his leg M2 turned around, looked down at M1 and then presented his back to M1 (presumably soliciting grooming) M1 huddled against M2 and both made lip-smacking gestures M1 then started grooming M2.	• *Alpha power:* Peaks in M1 IT, PFC and M2 IT. • *Beta power:* M1 beta power declining in IT, PMv, PFC and peaks in M2 IT. • *Partner decoding:* M1 > M2 at first, then M2 > M1 • *Joint models:* Partner > self for M1, no clear trend for M2. • *Partner neural model:* M1 > M2 • *Interpretation:* Initially M1 tracked his partner's identity and then M2 tracked his partner's identity. M1 is closely tracking his partner's joints, while M2 is tracking both his own & partner's movements. M1's brain activity is better predicted by M2, again indicating coupling.
385 to 388 s	M1 was grooming M2's face. M2 turned around to present his left shoulder to M1, and M1 responds by grooming there.	• *Alpha power:* Peak in M1 IT & PFC. • *Beta power:* Peak in M1 IT & PFC. • *Partner decoding:* Peak in M2 • *Joint models:* No clear trend but partner > self soon afterward in M2, and self > partner in M1. • *Partner neural model:* No clear trend but M1 > M2 soon afterwards. • *Interpretation:* M1 is relaxed (based on alpha power), M2 is aware of his partner's identity, and both monkeys are tracking the groomer's joint movements. M1 brain activity is predicted by M2, indicating coupling.

449 to 451 s	M1 was grooming M2's back M2 turned around to present his chest to M1, and M1 responds by grooming there.	• *Alpha power:* Peak in M2 IT. • *Beta power:* Peak in M2 IT. • *Partner decoding:* M2 > M1 • *Joint models:* No clear trends. • *Partner neural model:* M1 > M2 • *Interpretation:* M2 is tracking his partner's identity, and M1's brain is predicted by M2, indicating coupling.
480 to 482 s	M1 was grooming M2's right shoulder and stopped and looked downwards and touched M2's leg. M2 extended his right leg, presumably in response. M1 started grooming M2's right leg.	• *Alpha power:* Peak in M2 IT & PMv • *Beta power:* Peak in M2 IT & PMv • *Partner decoding:* M1 > M2 • *Joint models:* self > partner in both monkeys. • *Partner neural model:* M1 > M2 • *Interpretation:* M1 is tracking his partner's identity, M1 & M2 are tracking their own joints, but M1's brain is predicted by M2, indicating coupling.
520 s	M1 was grooming M2's foot. M2 starts grooming M1. M1 responds by stopping his grooming of M2.	• *Alpha power:* Peak in M1 IT, PMv, PFC soon afterwards. • *Beta power:* Peak in M1 IT, PMv, PFC soon afterwards. • *Partner decoding:* M2 > M1 • *Joint models:* partner > self for M2 and self > partner for M1. • *Partner neural model:* M2 > M1 soon afterwards. • *Interpretation:* M1 seems to relax (based on alpha power), M2 is aware of his partner's identity, and both monkeys are tracking the receiver's joints. M2's brain is predicted by M1, indicating coupling.
533 s	M2 is grooming M1 and making small changes in the groomed locations on M1's back without any obvious indications from M1.	• *Alpha power:* Peak in M1 IT, PMv, PFC. • *Beta power:* Peak in M1 IT, PMv, PFC. • *Partner decoding:* M2 > M1 • *Joint Models:* partner > self in M1, self > partner in M2. • *Partner neural model:* M2 > M1 • *Interpretation:* M1 is relaxed (based on alpha power), M2 is tracking his partner's identity, both monkeys are tracking the groomer's joints, M2's brain is predicted by M1, indicating coupling with receiver's brain.
570 to 572 s	M2 was grooming M1's middle back. M1 then lay down on the ground M2 responds by grooming M1's lower back.	• *Alpha power:* Peak in M1 IT, PMv, PFC • *Beta power:* Peak in M1 IT, PMv, PFC • *Partner decoding:* M2 > M1 • *Joint models:* partner > self in M2 at first, then partner > self in M1. • *Partner neural model:* M1 > M2

		• *Interpretation:* M1 is relaxed, M2 is tracking his partner's identity, M2 is tracking his partner's joints and then M1 is tracking his partner's joints, M1's brain is predicted by M2, indicating coupling with the groomer/dominant partner's brain.
625 to 628 s	M2 was grooming M1's lower back M1 starts touching his implant and licking his hand. M2 looks up to see what M1 is doing.	• *Alpha power:* No clear trend. • *Beta power:* No clear trend. • *Partner decoding:* low in M1 & M2. • *Joint models:* self > partner in M1, partner > self in M2. • *Partner neural model:* M1 > M2 • *Interpretation:* M2 is tracking M1's joints to see what M1 is doing.
633 to 638 s	M2 stopped grooming M1, who was lying down. M1 responds by getting up and turning to present his neck M2 responds by grooming M1's neck.	• *Alpha power:* Peak in M1 IT, PMv, PFC and in M2 IT. • *Beta power:* Peak in M1 PMv soon afterwards, Peak in M2 IT & PMv. • *Partner decoding:* M2 > M1 • *Joint models:* self > partner at first in M1, then partner > self, partner > self in M2. • *Partner neural model:* M2 > M1 • *Interpretation:* M1 is relaxed and M2 is relaxed, M2 is tracking his partner's identity, M1 is moving but also tracking his partner's joints, M2 is tracking his partner's joints, M2's brain is predicted by M1, indicating coupling with receiver's brain.
640 to 645 s	M2 holds M1's implant and bends M1's head to groom his right temple.	• *Alpha power:* Peak in M1 IT & PFC • *Beta power:* Peak in M1 PMv & later in M1 IT & PFC. • *Partner decoding:* M2 > M1 • *Joint model:* No data, since a few joints were not visible in the top view. • *Partner neural model:* M2 > M1 • *Interpretation:* M1 is relaxed, M2 is tracking his partner's identity, M2's brain is predicted by M1, indicating coupling with receiver's brain.

Table S2. Key neural events and the accompanying behaviors (ref: Figure S16)

Video Time	Summary of Ongoing Behavior	Key Neural Event
179 to 184 s	M2 was grooming M1's head M1 closed his eyes.	Key Neural Event • *Alpha power:* Peak in M1 IT, PMv, PFC. • *Beta power:* Peak in M1 IT, PMv, PFC. Other Neural Signals • *Partner decoding:* Drops for M1 Interpretation • *M1 is relaxed. Closing eyes is well-known to cause increased alpha power.*
235 to 260 s	M1 was looking up for a long time while M2 was grooming his neck.	Key Neural Event • *Alpha power:* Peak in M1 IT, PMv, PFC. • *Beta power:* Peak in M1 IT, PMv, PFC. Other Neural Signals • No clear trends. Interpretation • M1 is relaxed.
346 to 360 s	M2 looked at the roof while M1 was grooming his chin/neck.	Key Neural Event • *Alpha power:* Peak in M2 IT • *Beta power:* Peaks in M1 IT, PFC & M2 IT Other Neural Signals • *Partner decoding:* M2 > M1 Interpretation • M2 is relaxed but aware of his partner.

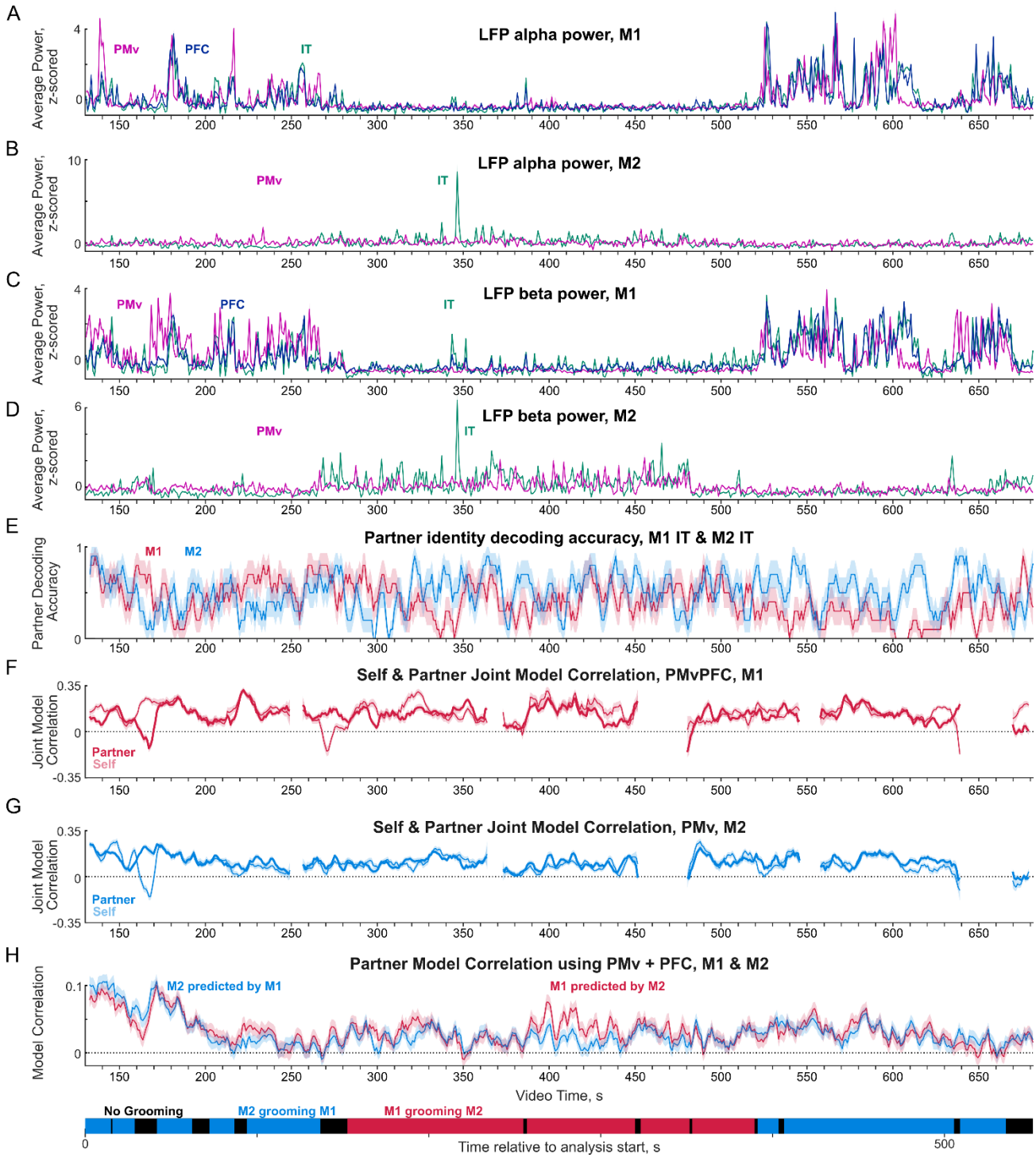

Figure S16. Convergent modulation of key behavioral & neural events

(A) Time course of average LFP power in the alpha band (8-12 Hz) for IT sites *(green)*, PMv sites *(purple)* and PFC sites *(blue)* in M1.

(B) Same as (A) for M2.

(C) Same as (A) but for beta band (12-30 Hz) in M1 sites.

(D) Same as (C) for M2 sites.

(E) Partner identity decoding accuracy, calculated in 5 s bins with a step size of 1 s from M1 & M2 IT (same as Figure S7).

(F) Instantaneous correlation (smoothed with a 5 s moving window with a step of 1 s) of the partner (*dark*) and self (*light*) joint models across PMv & PFC sites for M1. All conventions are as in Figure S10.

(G) Same as (F) for M2 PMv.

(H) Time course of smoothened partner model correlations for M1 & M2 during the entire interaction (same as Figure 6D).